Durham E-Theses

Extending Highthroughput Technologies: The Automation of Mechanism Discovery Investigations into the mode and action of the thio-Michael Reaction

WALTON, SIMON

How to cite:

WALTON, SIMON (2010) *Extending Highthroughput Technologies: The Automation of Mechanism Discovery Investigations into the mode and action of the thio-Michael Reaction*, Durham theses, Durham University. Available at Durham E-Theses Online: http://etheses.dur.ac.uk/237/

Extending Highthroughput Technologies: The Automation of Mechanism Discovery

Investigations into the mode and action of the thio-Michael Reaction

A thesis submitted to the University of Durham for the degree of Master of Philosophy

Simon Walton

Department of Chemistry, Durham University
Friday 22nd January 2010

Preface

To the best of my knowledge, the research described in this thesis is entirely original except where due reference is made and has not been previously submitted in support of an application for any other degree or qualification at this or any other university or institute of learning.

Simon Walton
Friday 22nd January 2010

Statement of copyright

Contents

Acknowledgements

perfer et obdura; dolor hic tibi proderit olim

Abstract:

This project concerns the investigation of the thio-Michael reaction (see scheme). The approach has employed a process development methodology to chemical discovery rather than more traditional research methods. Stage One involved the investigation of rates of addition with and without different catalysts to develop an understanding of the thio-Michael system.
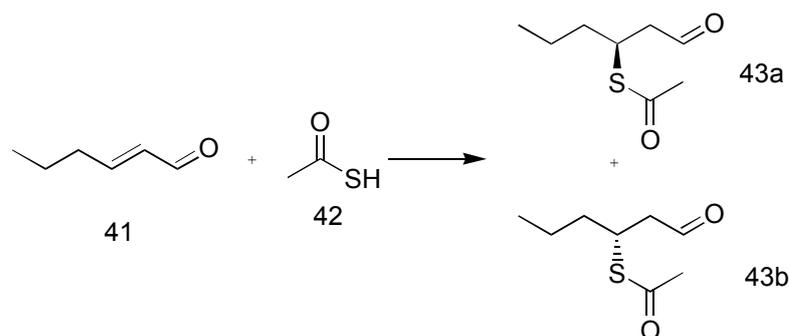
Further studies with asymmetric catalysts were carried out. Stage Two involved the use of adiabatic calorimetry and advanced reaction modelling to provide a complete understanding of the thio-Michael reaction under study. From this, the mechanism we propose is a new, self-accelerating process, in which the product may catalyse collapse of one observable intermediate to the product. The exact mode of this autocatalytic step is not clear at present, but is the subject of ongoing studies as is the generality of this new mechanistic insight into the Michael addition reaction.

Abbreviations List

Cp – specific heat capacity $(kJ.kg^{-1}K^{-1})$*

ρ - density $(kg.m^{-3})$

T – temperature (K)

t – time (s)

Qr – reaction exotherm (W)

Q_{loss} - rate of heat loss from the reactor (W)

Ri – rate of reaction i ($kMol.s^{-1}$)*

ΔH – enthalpy of reaction $(kJ.kMol^{-1})$*

k – rate constant $(m^{3}.kMol^{-1})^{n-1}s^{-1})$*

ϕ - phi factor (dimensionless)

m – mass (kg)

V – volume (m^{3})

C_j – concentration of species j $(kMol.m^{-3})$*

F – flow $(m^{3}.s^{-1})$

NMR – nuclear magnetic resonance

TLC – thin layer chromatography

IR – infra red

TMR – time to maximum rate

e.e. – enantiomeric excess

d.r. diastereomeric ratio

* Note: this project has been carried out in conjunction with chemical engineers. This unit of measurement is unusual for the chemist, but is preferred for large scale reactions.

1.0 Introduction

1.2 Background

The traditional approach to discovery is one of highly structured, repetitive series of experiments, geared towards a predetermined goal. History teaches us that it is often luck (or as scientists prefer to call it, thanks to Horace Walpole: serendipity) which is responsible for most of the major breakthroughs in science [1]. A search through the process development literature reveals further anomalies in the discovery process. A medicinal chemistry synthesis is altered by the process chemists and chemical engineers. The original synthesis has little or no consideration of health and safety issues or possible scale up issues. It is left to the process chemist to consider these issues, often much later in the discovery process. The Whitesides' Report [2] highlights the gap between chemistry and chemical engineering and encourages projects and collaborations that operate at this very interface and encourage the breakdown of traditional barriers.

It has been shown [3] that by bringing process engineers further upstream in the discovery process, the cost and time to market for compounds can be significantly reduced. Employing simulation and modelling techniques can rapidly help to fix on possible synthetic routes, saving the experimentalist valuable time.

This introduction will be in two parts, the first concerning the chemical engineering background, and the second providing background on relevant chemistry.

1.3 The Chemical Engineering Approach to Mechanism Discovery

The most important factor for a chemical engineer to bring a material to large scale production is safety. The plant must be able to cope with the process and the chemistry process must be fully understood from the view point of thermodynamics and kinetics to potential crystallisation routes, or distillation columns. The results of poor understanding can be dramatic [4].

1.3.1   Adiabatic Calorimetry

Adiabatic calorimetry is a particularly useful probe for chemical reactions. Under the worst industrial real case scenario; external cooling is lost on a reactor while an exothermic reaction proceeds. Essentially there is no heat exchange with the surroundings and the reactor can now be considered to be under adiabatic conditions. When a chemical reaction produces more heat than the heat loss from the system it is said to "runaway" [5]. Most chemical reactions follow an Arrhenius Law where

$$Rate \propto Z.\exp(-E_a / RT) ;$$ Eqn 1

Thus the temperature is part of the exponential term
however the heat transfer across a reactor is only

$$Rate = U.A.(T_j - T_r).$$ Eqn 2

i.e. proportional to temperature
The effects of this are described by Semenov [6] (stirred reactor) or by the Frank Kamenetskii Theory [7] (unstirred reaction). Given that thermal runaway can have very dangerous consequences it can now be appreciated that studying an exothermic reaction under adiabatic conditions is a sensible safety precaution.

1.3.1.1 Φ Factor

In order to study adiabatic behaviour an understanding of the reaction vessel is required. When an exotherm occurs both the sample causing the exotherm increases in temperature as well as the vessel the sample is contained in. When monitoring the temperature rise in

an adiabatic system, the vessel's properties must be taken into account for a true picture of the system under study. In order for the data to be meaningful there must be a compensation factor for the vessel. A jacketed vessel, containing an exothermic reaction, absorbs heat from the surroundings and the reaction, and emits heat to the surroundings or thermoregulation system around it. The material of construction (amongst other factors) contribute to the rate at which this heat energy is transferred. This compensation factor is described below:

$\phi = $ <u>Thermal mass of sample and test cell</u>　　　　　　　　　　　　Eqn 3

　　　　Thermal mass of sample alone

$$\phi = \frac{m_{reagent}Cp_{reagent} + m_{reactort}Cp_{reactor}}{m_{reagent}Cp_{reagent}}$$　　　　　Eqn 4

The Φ factor describes the thermal mass or thermal inertia of the reactor (i.e. its resistance to increasing its temperature). It is important to note that on small scale the thermal mass of the vessel is a much larger fraction of the total thermal mass than on large scale; also that the Φ factor can be applied to storage vessels, distillation columns, etc. Most large chemical plant reactors have Φ values between 1 and 1.05.

1.3.1.2 Φ Factor Corrections

Since

$$C_p\rho dT/dt = Q_r$$　　　　　Eqn 5

$$\phi C_p\rho dT/dt = Q_r$$　　　　　Eqn 6

Equation 5 describes the classical relationship between the total energy of the system and is modified to take account of the reactor vessel in equation 6 as discussed above.

A Φ factor close to 1 is ideal for a calorimeter as the kinetic and thermodynamic parameters can be determined from classical equations (assuming Arrhenius dependency). If the Φ factor is greater than 1 then correction factors need to be applied

to elucidate the system. These corrections are described by the theory of Townsend and Tou [8], which describe the corrections needed when vessels have very large or very small Φ factors and the mathematical details are outside the scope of this work.

1.3.1.3 Information Required

Adiabatic calorimetry can now be used to answer the following questions:

- Thermal behaviour (is there a thermal hazard in the event of loss of cooling?);
- Onset temperature (what temperature is a thermal event detected?);
- Induction time (how long to TMR, time to maximum rate?);
- Temperature rise (what is the maximum temperature that the vessel will experience under adiabatic conditions?);
- System characterisation (is a pressure rise due to vapour pressure or a gas product?);
- Rate of change of temperature (are there multiple reactions and what are their kinetics?);
- Rate of change of pressure (how fast is the pressure rise and is it pressure dependent?)

1.3.1.4 Methods Available [5,11]

There are numerous methods for answering these questions ranging from the use of simple equipment to complex computer controlled equipment.

- Dewar flask: good for low pressure systems, and readily available from domestic suppliers. This can be modified by introduction of probes and sensors depending on vessel type.

- Accelerating Rate Calorimeter (ARC): a small bomb vessel with external heaters. The Φ factors are often high. The external heater is slaved to the internal

temperature probe to ensure adiabacity. The cell can rupture, however high sensitivity is possible.

Figure 1 Selection of ARC Bombs

- VSP – PHITEC – APTAC: all three operate in very similar manners. VSP (vent size package) is manufactured by Fauske; PHITEC (Phi [factor] technology) is manufactured by HEL; APTAC (automatic pressure tracking adiabatic calorimeter) is a generic name. A low thermal inertia vessel is maintained inside a larger pressure vessel with a pressure feedback loop to prevent vessel rupture. These machines can be time consuming and difficult to operate.

Figure 2 APTAC Containment

- Reactive System Screening Tool (RSST): although non-adiabatic, and reliant on constant small heat inputs to compensate for heat losses, etc. the method seems to give good (if conservative) results. True adiabatic testing may be needed.

Figure 3 Reactive System Screening Tool, with computer interface

1.3.2 Kinetic Regression

Bhattacharya[9] sets out a mathematical framework for mass and energy balances in an adiabatic calorimeter. This requires the user both to develop and solve the differential equations. For those not trained in chemical engineering and in particular modelling and numerical solutions this may be an onerous task.

1.3.2.1 Kinetic Modelling

Although the use of adiabatic calorimetry is not commonly reported for kinetic rate regression and by implication reaction mechanism, it may prove to be very effective when used in conjunction with powerful kinetic modelling software such as BatchCAD™[10]. This is particularly the case for the Dewar reactor for which it is difficult to maintain the external temperature of the flask to that of the contents and heat losses inevitably occur.

BatchCAD™ employs an intelligent syntax analyser to interpret chemical reactions, physical properties, plant details and user specified operating conditions to both automatically construct and solve rigorous dynamic mass and energy balances.

Thus for *m* chemical species involved in *q* reactions with *n* feed streams and *p* streams leaving the system the mass balance equation is

$$V \cdot \sum_{i=1}^{m} \frac{dC_i}{dt} = \sum_{i=1}^{m} \left(\sum_{j=1}^{n} F_j \cdot c_{iF_j} - \sum_{k=1}^{p} F_k \cdot c_i + \sum_{l=1}^{q} R_l - c_i \cdot \frac{dV}{dt} \right) \qquad \text{Eqn 7}$$

Similarly a general energy balance is written

$$V \cdot Cp \cdot \rho \cdot \frac{dT_R}{dt} = \sum_{j=1}^{n} F_j \cdot Cp_{F_j} \cdot \rho_{F_j} \cdot \left(T_{F_j} - T_R \right) + UA \cdot \left(T_W - T_R \right) +$$

$$\sum_{l=1}^{q} \Delta H_l \cdot R_l + m_{reactort} Cp_{reactor} + Q_{loss} \qquad \text{Eqn 8}$$

where Cp is specific heat and ρ is the density (of the system under study). The reaction enthalpy is ΔH. T is temperature and the subscript R denotes reaction mass and W the vessel wall. In simple terms these equations (7 and 8) allow a mathematical description of how the thermodynamics of the entire system are affected by altering the rates of addition, the differing temperatures of the addition streams and reactor contents, the removal of material from the system, the effects of external heating or cooling, and subsequent heat loss or gain from the surroundings.

The following correspond to the various mechanistic steps in the reaction scheme:

$$Qr = \sum Ri \Delta H_i \qquad \text{Eqn 9}$$

$$R = k[\text{Pr} oducts]_{init} \qquad \text{Eqn 10}$$

$$k = Z \exp(-E_a / RT) \qquad \text{Eqn 11}$$

These mass and energy balances are solved by BatchCAD™ either separately or simultaneously for either process simulation or kinetic regression. In the latter case by the determination of isothermal rate constants, Arrhenius constants and reaction orders for complex reaction networks from measurements of composition, temperature and heat

flow. In simple terms (the complex information is proprietary) BatchCad compares the integration of the experimental data with the integration of the predicted data. Using an 'intelligent analyser' the software then adjusts the variables in the model until a good fit is obtained between the experimental and predicted data.

1.3.3 Adiabatic Calorimetry as a Reaction Probe

As discussed earlier in section 1.2.1, calorimetry is an often necessary study of a reaction before it can proceed to plant-scale synthesis. The implications of poor understanding of reaction dynamics and the subsequent runaways, explosions and casualties litter the process safety literature. The following section highlights both safety issues and subsequent reaction engineering allowed by a thorough understanding of the thermodynamics of the system.

1.3.3.1 Thermal Hazard Assessment

As an example preparation of Grignard reagents on large scale can be problematic due to initiation problems caused by poor reactivity of the substrates, surface oxidisation of the magnesium metal, poor moisture control and other factors. A new alternative has recently emerged using a magnesium-halide exchange reaction, where a pre-existing solution of i-PrMgCl is reacted with the substrate in question to form the Grignard reagent required at -20 °C as a homogeneous solution[9]. A recent study by Boehringer Ingelheim Pharmaceuticals Inc.[10] shows that for even simple substitution reactions (scheme 1) there is a significant thermal hazard if cooling is removed. The reaction onset temperature is 80 °C, with a peak temperature rise rate of 410 °Cmin^{-1} reaching a maximum temperature of ~210 °C.
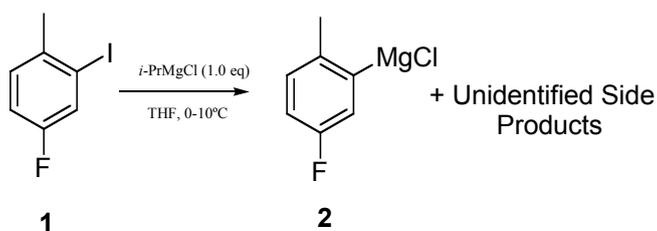
Scheme 1: magnesium-halide exchange reaction with iodotoluene and *i*-PrMgCl

The by-product of *i*-PrI in the reaction is not simply an inert species in the reaction and the suggestion is that it opens decomposition pathways for the other species. This exotherm would not have been noticed unless chemical engineering rigour had been applied to the system.

1.3.3.2 Mechanism and Kinetics

The simplicity of adiabatic calorimetry as a reaction probe is highlighted by the Glasser group[12], by using it to probe the base catalysed aldol condensation of acetone. This particular reaction is difficult to probe due to the small conversion (ca 1%). In the past the reaction has only been directly studied once by using very sophisticated equipment[13] and Glasser's work has thrown doubt on this work due to the use error in the data used for the exponential curve-fitting. The reaction has also been probed by inference from the backwards reaction by other groups[14]. The results from the reaction show the equilibrium constant for the ionisation of acetone to be 1.2 dm^3 mol^{-1} and the rate constant for the rate-limiting addition step to be 2.5 $\times 10^{-3}$ mol dm^{-3}, all of which are in agreement with the classical work[14] though not in agreement with discounted direct study.

Merck have recently used calorimetric methods to probe the safety implications and mechanism for a Leimgruber-Batcho indole synthesis as an intermediate for a drug candidate[15]. Scheme 2 shows the reaction under study.
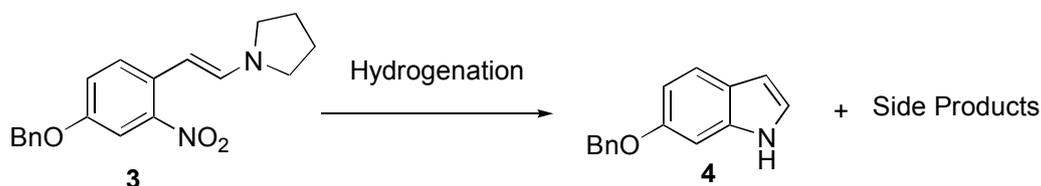
Scheme 2 Synthesis of drug intermediate

The initial synthetic step was a reduction of **3** using Raney nickel in EtOH, with addition of hydrazine as the hydrogen source. Adabatic calorimetry (using a reaction calorimeter operating under adiabatic conditions) revealed that not only were there delays in the exotherm, but that the exotherm could raise the system above the boiling point of EtOH if the cooling unit failed. The group recently reported a small scale synthesis of this intermediate **4** using Rh/C with H_2 and additives to minimise the unidentified side-products [16]. The only question was whether the new process was scalable and safe. Screening studies revealed the addition of Fe(acac)$_3$ reduced the side products and on laboratory scale gave a yield of 96%. On scale up (20-L autoclave) the yield was 88%.

The Blackmond group at Imperial College UK, have been using calorimetric methods for some time to study reactions and mechanisms. In particular their work involves using thermochemical methods to deduce reactions networks and then translation into putative chemical mechanisms. The limitation of this work is that the thermochemistry is used in isolation. Other classical methods e.g. UV-VIS kinetic studies are used for determining non-thermodynamic parameters, as opposed to using an integrated approach as described earlier in §1.2.2. However, the group has had success probing various catalytic systems, e.g. proline catalysis and Pd mediated cross-coupling reactions. Studies of various aldol and aldol-type reactions using L-Proline as the catalyst as well as other amino acids have shown some interesting non-linear effects. Of particular interest to scientists in general is the non-linear observations in enantiomeric excess, leading the authors to suggest a possible link to homochiral evolution[17]. Other work also shows non-linear effects in e.e.; as well as non-linear rate effects determined from the heat rise profile[18].

In the area of metal mediated catalysis, the Blackmond group has also had success using similar methods. Catalyst screening is often a difficult and time consuming process, especially if detailed kinetics are required. By using a heat flow approach it is possible to screen catalysts in a single pot reaction. By using high concentrations of substrates, pseudo-zero-order kinetics will be established and the rate constant k′ will be amplified over the intrinsic rate constant *k* since is incorporates the excess initial concentrations of the substrates.

$rate = k' = k[A_0]^x[B_0]^y[cat]$　　　　　　　　　　　　　　　　　Eqn 12

With the reaction operating under pseudo-zero-order conditions, small injections of the different catalysts under study will result (given certain preconditions) in a step wise heat flow graph, and the kinetics are directly related to the heat flow. The Blackmond group have used this method to speed up the catalyst screening for the asymmetric hydrogenation of Z-α-acetamidocinnamic acid[19].

1.4 The Chemistry of Michael Additions

The basis of the experimental work for this thesis is an investigation into the Michael Reaction. This section will discuss the various types of catalyst that can be used in Michael additions which will lead to the Results section where the specifics of the thio-Michael reaction will be discussed. Some of the catalytic methods discussed in this section are applied to system under study with subsequently surprising results which are explained by a detailed investigation of the kinetics and mechanism of the reaction.

1.4.1　Introduction

The Michael addition is one of the oldest[20], most important and widely used reactions in organic chemistry[21]. Over a number of years it has been sufficiently well studied that important aspects such as regio- and stereo-control, and the control of absolute stereochemistry seem to be well understood[21]. The broadly accepted mechanism of the Michael addition reaction involves a direct addition of a nucleophile to the remote carbon of the conjugate system[22]; a view which has changed little since its discovery. The utility of the Michael process is a direct result of its broad applicability in terms of both electrophile and nucleophile, with hetero-Michael reactions[23] being thoroughly investigated and exploited for accessing β-oxy-, aza- and thio- carbonyl compounds from unsaturated carbonyl derivatives.

11

1.4.2   Organocatalysis of Michael Additions

Organocatalysis is a rapidly developing area [24], examples of which were reported a few decades ago [25], however, more general and efficient enantioselective methods have been recently developed [26]. The recent upsurge in organocatalytic methods, *i.e.* catalysis without the use of a metal centre [27], stems from several positive environmental benefits, including the reduction in heavy metal waste [28]. Michael and hetero-Michael additions [29] are widely used in synthesis, being important bond forming reactions including asymmetric catalysis [30].

1.4.2.1 Urea Type Catalysts

Catalysis of the Michael reaction can occur through 2 different interactions, the catalyst with the Michael acceptor, or with the Michael donor. Urea and thio-urea groups are known to coordinate to the carbonyl group of the acceptor and lower the LUMO energy via partial protonation. As can be appreciated, development of these types of catalysts is the subject of much research [31]. Employing the same logic, guanidine based catalysts would also be a useful set of structures to explore. The Nagasawa [32] group in Tokyo have explored various types of catalysts based on these central motifs, of which **5** and **6** are the most active:

5: X = O
6: X = S
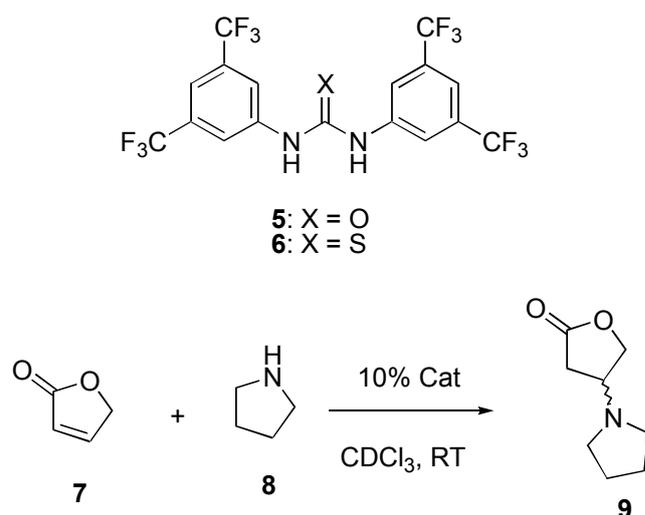
Scheme 3 catalysing the reaction of pyrrolidine with γ-crotonolactone

5 and **6** offered a relative rate increase of >24 fold over the background reaction. Applying a chiral amine linker between two urea groups gives access to a series of chiral catalysts.
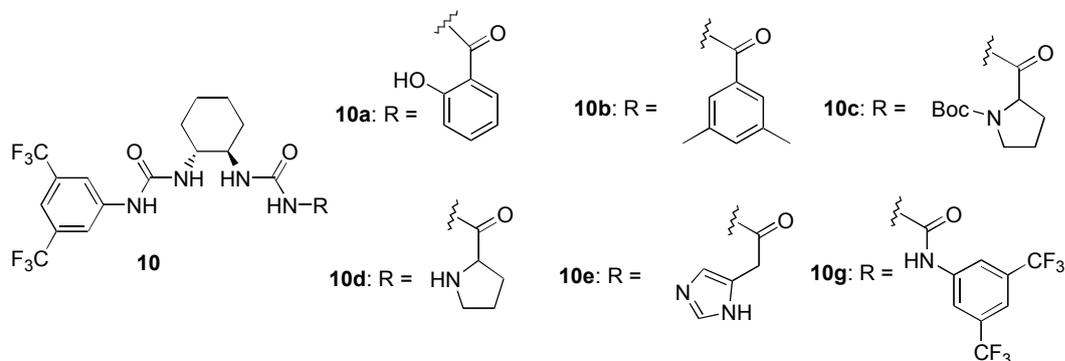
Unfortunately the relative rate increase was no greater than 10 fold, and the e.e. was disappointing ranging from 0 - 19% depending on solvent and temperature.

The Jacobsen group has for some time been investigating organocatalytic systems, in particular bifunctional type catalysts. Their urea based catalyst [33] **11** has shown high activity with yield and e.e. >99%, and a d.r. >10:1
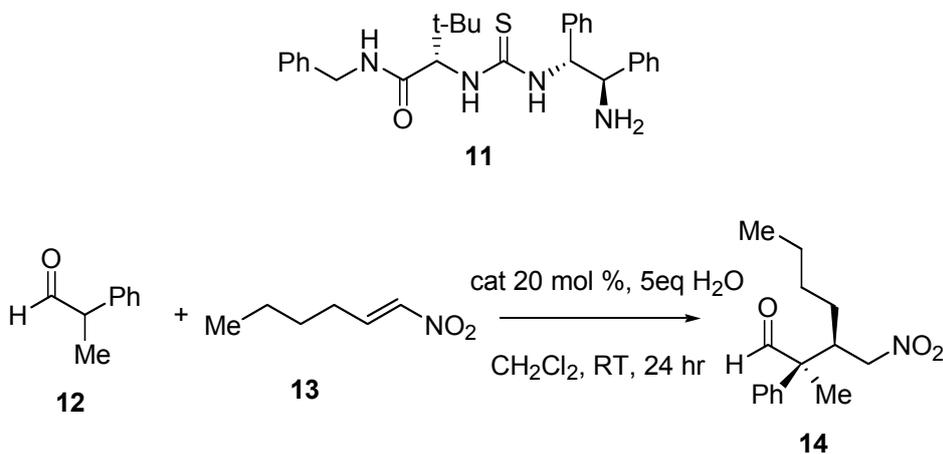
**Scheme 4** Catalyst **11** shows high activity

The group speculates that the mechanism goes through the thermodynamically more stable E enamine which accounts for the diastereoselectivity.

13

These conceptually similar examples show a good series of organo-catalysts, with the thio-urea type being most effective in both rate increase and selectivity. However, recent literature in this area has been dominated by proline and proline derivative potential catalysts.

1.4.2.2 Proline based Catalysis

Proline[34] has been used for catalysing many reactions including the aldol condensation, and other reactions where enamine intermediates are possible (scheme 5). Furthermore, as part of the chiral pool, L-Proline is cheap and readily available and the amine and acid groups are available for varied functional group conversions to allow access to other structures and subsequent optimisation of the catalytic functions.

The List group, while known for aldol type reactions have looked at the Michael reaction as well. Michael addition with amine based catalysts can potentially go through two mechanisms, iminium or enamine pathways as shown in scheme 5

Iminium Pathway   Enamine Pathway
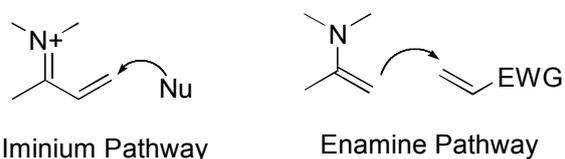
**Scheme 5** Mechanistic possibilities for the Michael Addition

The enamine pathway was previously unreported. However the List group [35] have been able to show that such a pathway is possible with the following reaction:
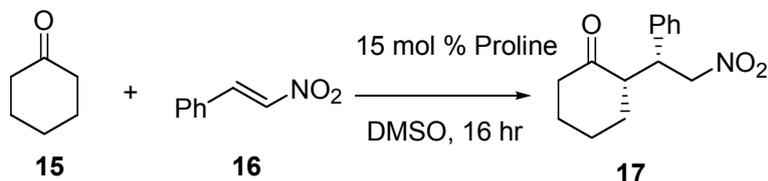
Scheme 6 Addition of an unmodified ketone to a nitro-olefin

Although the reaction is high yielding (typically >90%) the diastereoselectivity is extremely poor. The group claims high hopes for the development of further catalysts, but this, has so, far not been reported.

Similar work has been continued in Japan by Hayashi, who has used the same principle to greater effect[36], achieving high yields, >90% e.e. and high *syn/anti* ratios. Prolines, modified by siloxy groups are known to be effective catalysts, and **18** was used in great effect:
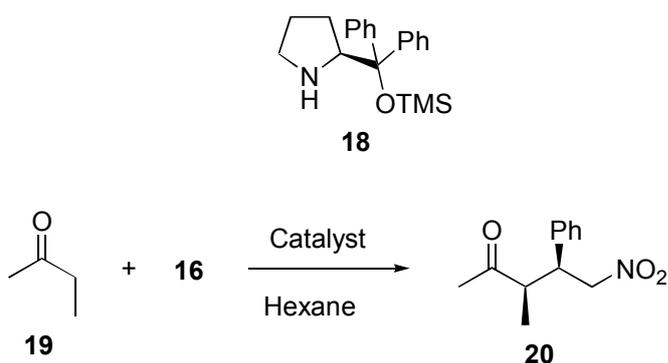
Scheme 7 High e.e. observed

As observed by List, and shown by this group the activation of the substrate is highly substrate sensitive.

There is not a large amount of literature for hetero-Michael additions utilising proline as a catalyst, however the Jørgensen group, driven by their interest in biologically active molecules has developed and efficient methodology for addition of *N*-heterocycles to unsaturated carbonyl compounds. These types of molecules have been shown to have important biological properties [37], and 1,2,4-triazoles and tetrazoles are important motifs in drugs such as Voriconazole (VFend™), Fluconazole (Diflucan™) and Losartan (Cozaar™). The catalyst was very similar to **18**, however, the phenyl groups were replaced by the $3,5\text{-}(CF_3)_2C_6H_3$ moiety. The catalyst shows good to high activity and e.e. >90%. The group has further proposed a catalytic cycle based on DFT calculations for the reaction [38]:
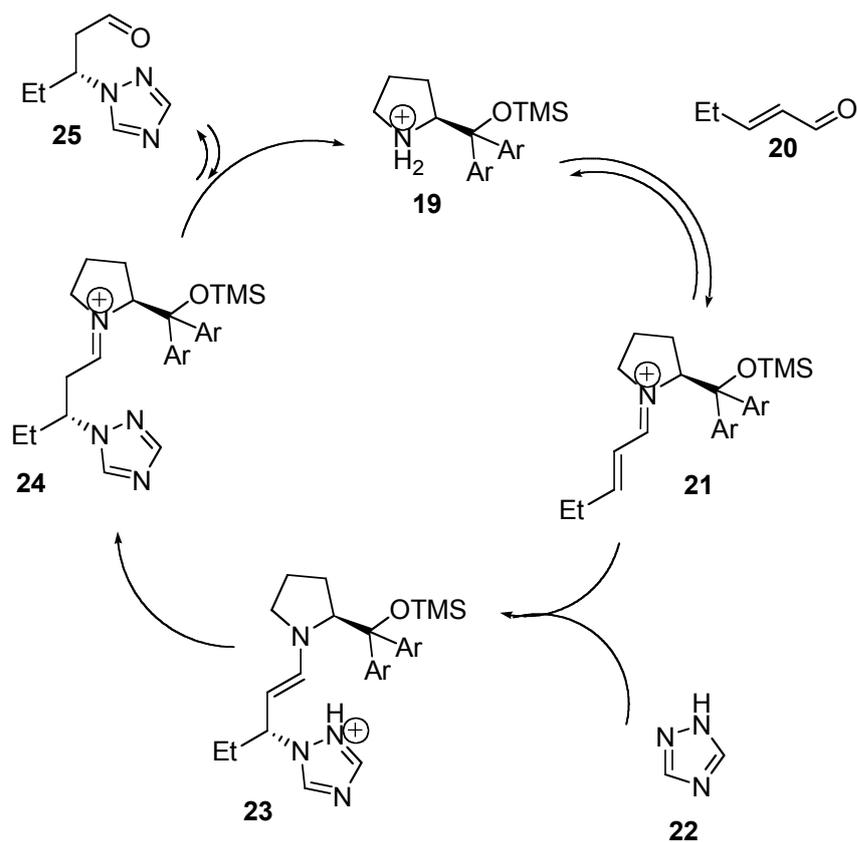
Scheme 8 Proposed mechanistic scheme, supported by DFT calculations

1.4.2.3 Multi-Component Reactions (MCR)

The mechanism of the Michael addition is accepted as the attack of a nucleophile on the remote carbon of the conjugated double bond system, followed by a keto-enol tautomerisation to return the carbonyl group. If the keto-enol tautomerisation is considered a separate reaction; it is not a great leap of the imagination to realise that the electrophile does not need to be a proton, but any electrophile will suffice.
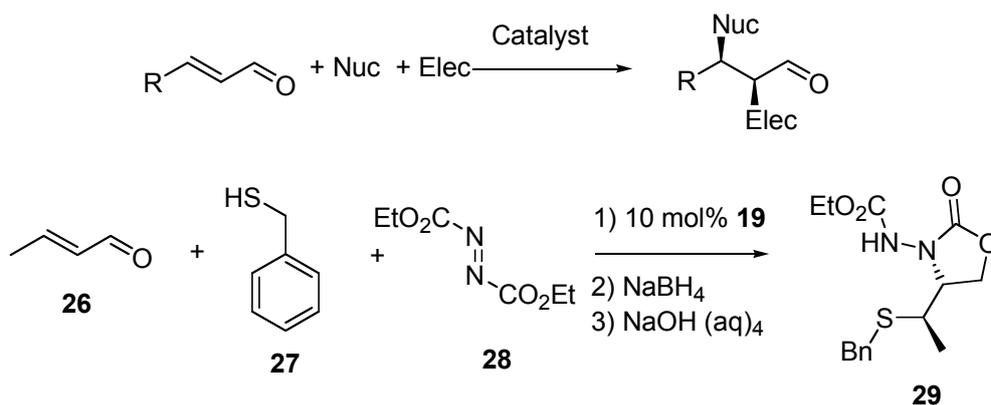
Scheme 9 Principle of MCR, with example

The Jørgensen group again using their proline derived catalyst **19** have achieved good yields and enantioselectivities; 80% and >95% respectively[39] by using thiol **27** as the nucleophile and DEAD **28** as the electrophile.

1.4.2.4 Other amine based catalysts

N-i-Pr-2,2′-bipyrrolidine is known to catalyse the addition of aldehydes and ketones to nitrostyrene **16**, in good to excellent e.e. and high d.r.[41]. This catalyst has also been used to give the first Michael additions of aldehydes to vinyl sulfones with reasonable yields and moderate enantioselectivities[42].

Cinchona alkaloids and their derivatives have also been used effectively for the hetero-Michael reaction: addition of thioacetic acid[43] (as well as *N*-heterocycles) to nitrostyrenes[44]. Both of these proceed in good yield with good enantioselectivities, and are some of the few non-auxiliary induced (organocatalytic) examples of the thio-Michael reaction.

1.4.2.5 Chiral Auxiliary induced synthesis

The direct, organo-catalysed addition for the thio-Michael reaction is relatively poorly described in the literature; however there are a few examples of chiral auxiliary induced synthesis. For the process chemist, auxiliary based chemistry is not appealing due to the

extra steps required and the potential for poor atom economy. However the chiral auxiliary approach has provided a few examples: the addition of thioacetic acid[45] and methyl thiol[46] have been shown to proceed in high yield and high enantioselectivities.

1.4.3 Metal Mediated Michael Additions

Having discussed the organo-catalysed systems the following sections will look at metal mediated catalysis of the Michael Addition.

Owing to the diversity of potential metal mediated and metal catalysed systems, the following has been split into high-MW metal and low-MW metal sections, where the subject relevance is on the metal rather than the potential ligand.

### 1.4.3.1 Low MW Metal mediated processes

Depending on the particular substrates for the Michael addition, enolates often need to be generated for the homo-coupling. Deprotonation by a strong lithium base allows access to the lithium-enolate, which can then react onwards with the desired substrate to give the Michael product.
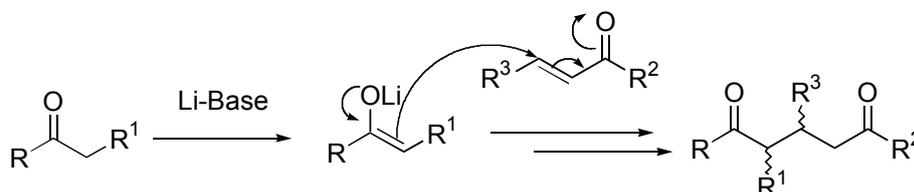
Scheme 10 General mechanism for Li-enolate Michael additions

The deprotonation stage can, of course, cause problems because depending on R^1 and R^2 there may be another hydrogen which could be removed by the base, leading to undesired side products. The reactions are mostly carried out at -78 ℃ as at higher temperatures 1,2 addition can occur[47].

Depending on the size of the R groups and the relative size of the 'OLi' group, the *syn/anti* ratio will differ.
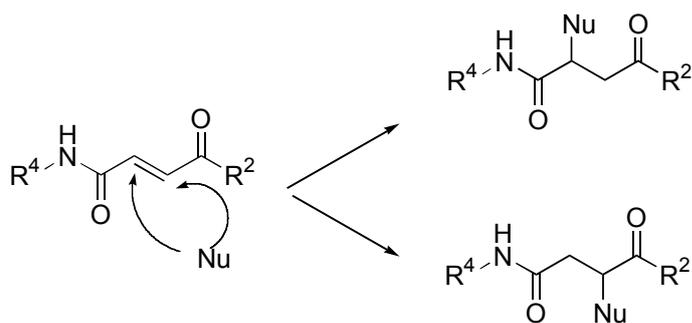
Scheme 11 Potential products in the case of unsymmetrical acceptors

This is explained by the Felkin-Ahn projection of the molecule:
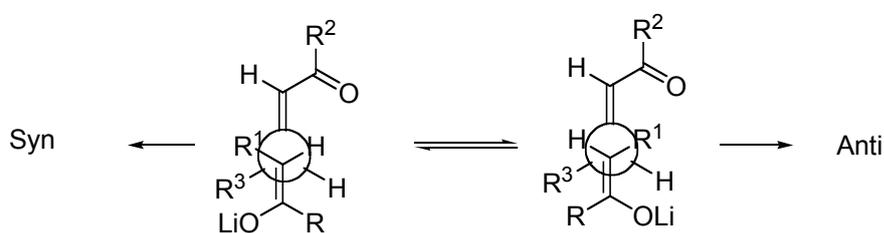
Scheme 12 Felkin-Ahn Projection (based on Scheme 10)

A recent study[48] has highlighted these potential issues during a study into the addition of thiols to unsymmetrical fumaric derivatives (scheme 13). The authors show that reaction conditions, in particular the form in which the thiol is used (lithium thiolate, or as the free thiol with other additives) is critical to controlling the regioselectivity.
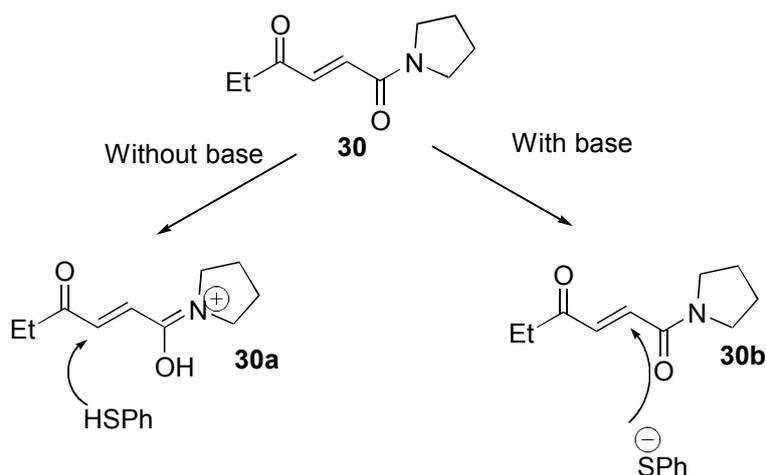
Scheme 13 Routes and implied products for addition, depending on conditions

DFT calculations support the experimental results. Using this approach the group then proceeded to use the sulfur moiety as a leaving or activating group to allow access to various other structures including lactams and lactones. The relative stereochemistry is dependent on the original regiochemistry of the sulfur group.

Construction of rings using Michael additions is of particular interest as the products can give access to potentially novel structures with highly functionalised rings systems. This use of vinylic sulfoxides as Michael acceptors are well known[49], however, their use (even though α-deprotonation is known[50]) as 'Michael donors' has remained relatively unexplored. Until recently there were only a few examples[51] which suffered from very poor diastereoselectivities, except for one example[52]. The Tanaka group in Japan has, however, made great progress in this area[53,54].
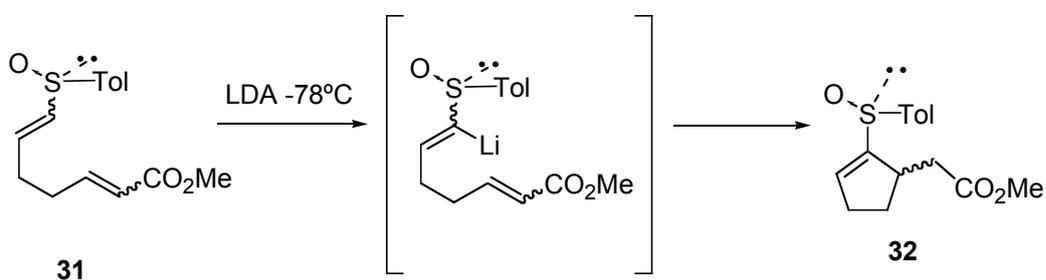
Scheme 14 α-sulfinyl vinyllithium Michael donor and subsequent cyclisation to the target molecule

In two papers the group has demonstrated the versatility of this method, which allows for larger rings to be synthesised[53], as well as high diastereoselectivities[54]. However, the (Z)-enolates gave R-configuration at the β-position of the ester in the 5-ring system, and this was reversed in the generation of the 6-ring product. The group proceeded to further functionalise the product and demonstrated the irreversibility of the Michael addition by treatment of the cyclised products with LDA and no retro-Michael or epimerisation observed.

BINOL **33** is well known as a ligand for many metals in organic synthesis. The drawback to many of these compounds is in the reliance on heavy metals and their instability to oxygen and moisture (see § 1.3.3.2 for references and examples for the Michael reaction). An Indian group[55] has recently developed calcium-BINOL **34** for use in asymmetric Michael Additions (Scheme 15), and it gave good to excellent yields for the addition of various malonates to cyclic and acyclic enones, with moderate to good enantioselectivities. Interestingly, the use of this catalyst did not lead to any e.e. for the addition of thio-phenol to cyclohexanone.
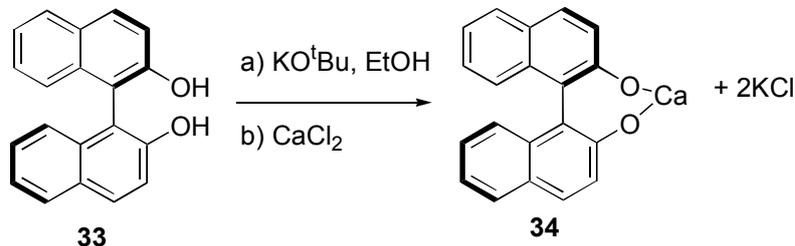
Scheme 15 Production of calcium-BINOL

Engineering implications aside, heterogenous catalysts are of interest to the process chemist due to the inherent ease of the catalyst: recovery, reusability and possibilities for operating the process continuously. A recent report from China demonstrates the use of a KF/Al$_2$O$_3$[56]catalyst for range of Michael additions of *N*-heterocycles, thio- and oxy-Michael donors, as well as sulfonamide formations to ethyl acrylate as the Michael acceptor[57]. Reaction times at RT were of the order of 18-24 hours, and the yields are reasonable to excellent. The exceptionally mild conditions (though unfortunate use of

solvents – DMF (high boiling and toxic/tetragenic) and MeCN (toxic and difficult to remove from material) - offer promise for this system on scale. However, the question of whether this technology could be developed for an asymmetric system is still open to question.

1.4.3.2 Higher MW Metal mediated processes

The aza-Michael reaction has synthetic interest as it provides a route to β-amino acid derivatives. Various transition metals have been screened in a high-throughput manner for the addition of amines to acrylic acid derivatives [58] for the production of β amino acids. In a recent paper[59], there has been progress in the direct addition of amines to unsaturated, activated, conjugated systems.
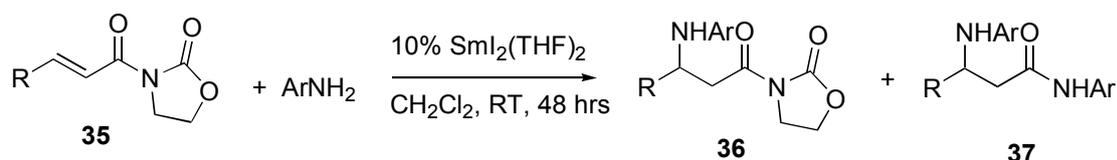
Scheme 16 Use of a samarium iodide complex as an effective aza-Michael catalyst

The reaction produced either singly (generally greater than 70%) or a mixture of β-*N*-acyloxazolinones or β-amino acids. Unfortunately, the paper offers no explanation for avoiding undesired products, or switching the outcome of the reaction, it does, however, comment that the likely cause is the differing electronic natures of amines. Further work is underway investigating asymmetric versions.

Combining two different Lewis acids – to form potential heterobimetallic catalysts are not new and reports have existed of their catalytic properties since the 1990's[60]. The Shibasaki group has gone on to develop further catalysts based on the rare earth metals (RE), alkali metals (M) and BINOL (B) – so called REMB catalysts:
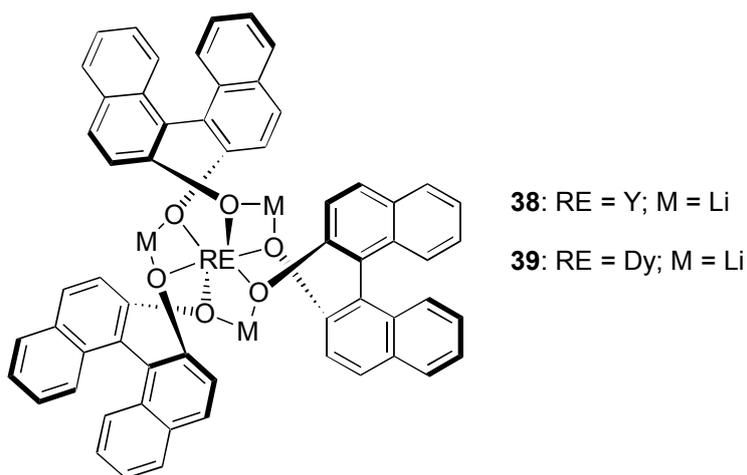
Figure 3 – examples of an REMB catalyst

38: RE = Y; M = Li

39: RE = Dy; M = Li

The Shibasaki group[61] decided that this catalyst type might be suitable to operate in a co-operative Lewis acid – Lewis acid manner, for the aza-Michael reaction. The amines of interest were *O*-alkylhydroxylamines and it was envisaged that the oxygen of the amine would coordinate to the metal, without effecting the nucleophilicity of the nitrogen. As such the following reaction was screened
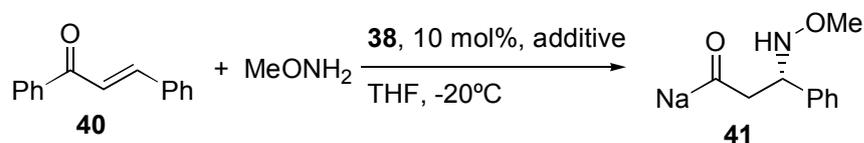
Scheme 17 Example of additive screening reaction

Although water did not affect the entantioselectivity of the reaction it did retard it, and as such, various drying agents were tried, including molecular sieves and Drierite ($CaSO_4$). The optimal conditions used Drierite and 0.5 mol% catalyst however this did give a reaction time of 80 hours (96% yield and e.e.). The scope of this reaction is particularly broad with most combinations giving >90% yield and enantioselectivities of the range 80-96%. The poor results using crowded amines suggest that complexations are important in the catalytic cycle, and amines without an oxygen group also gave poor results. As such the group postulate the following cycle:

23
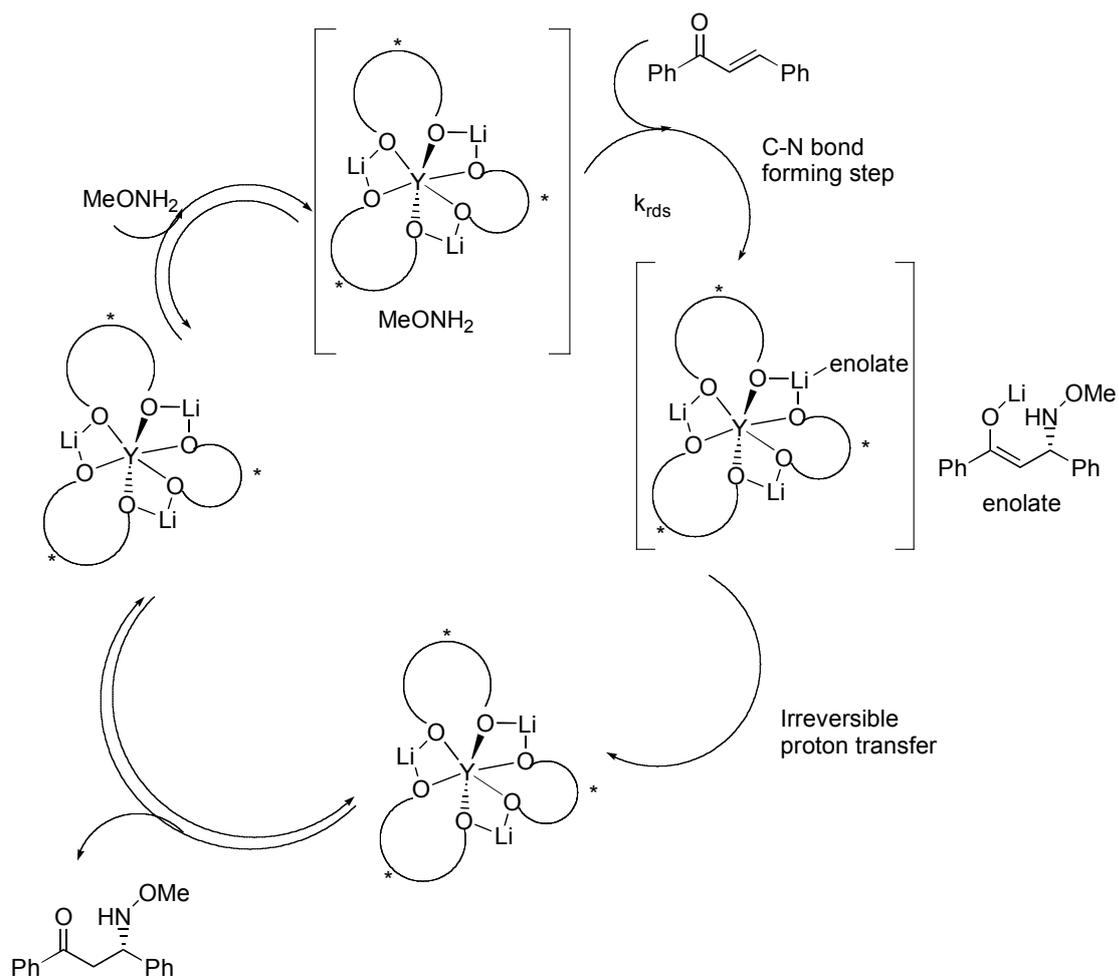
Scheme 18 Postulated catalytic cycle

Other rare earth metals were screened and the best e.e.s were observed with Y and Dy. Also, positive nonlinear effects were observed for enantioselectivity and negative nonlinear effects for reaction rate.

Copper tetrafluoroborate has also been used to catalyse the use of thiols as Michael donors, in good yields with a variety of cyclic and α,β-unsaturated ketones, in water at room temperature, with the reactions proceeding in under an hour, with yields greater than 90%[62].

1.4.3.3 Other systems

Fixed or heterogenous catalysts are always of interest to the process chemist, and a recent report described the use of Cu-Al hydrotalcite to efficiently catalyse the aza-Michael addition of amines to methyl acrylate, acrylonitrile and methyl vinyl ketone. The reactions proceed efficiently and the catalyst was recoverable, and could be reused without significant loss of activity and negligible metal leaching[63]. In a similar manner benzenethiol has been added to various cycloalkenones using a faujasite catalyst which operates in a simultaneous acid-base bifunctional manner[64]. The reactions proceed with yields in the range of 64-89%, however disulfide formation can be problematic.

Any catalyst that can be polymer-supported is also popular in the literature and $[HP(HNCH_2CH_2)_3N]NO_3$ has been shown[65] to promote the aza- and thio-Michael reactions with yields often in excess of the non polymer-supported catalyst reaction. The ammonium salt has also been bound to a Merryfield resin, and again produces excellent yields, and is recyclable upto 20 times without loss of activity. The catalyst has also been used on the Strecker[66] reaction as well as 3 and 4 component reactions.

Iodine has also been used to catalyse the addition of pyrroles (useful intermediates for drug candidates as mentioned earlier) to unsaturated ketones[67]. The main draw back of this method was the appearance of the dialkylated product.

Borax has also been used to catalyse the thio- and aza-Michael reaction with excellent yields (85-96%) in aqueous media[68].

2.0 Results and Discussion

2.1 Origins of the Project

25

The following Michael addition is of interest synthetically and commercially:
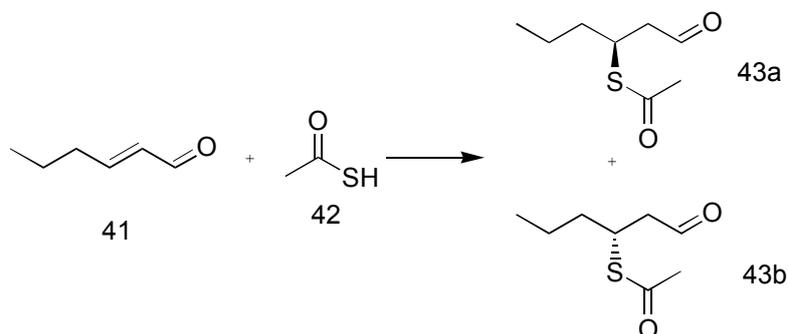
Scheme 18

The *R* and *S* enantiomers, **43a** and **43b** respectively have potentially important applications in the flavourings and aromas industry. At present there is no literature which shows any enantioselective methods of making these compounds other than by enzymatic resolution. As such our collaboration with Oxford Chemicals is looking at methods to synthetically produce pure enantiomers of this and related compounds. This reaction will be discussed later in more detail.

The enantiomers of **43** have been reported as flavour compounds in cooked liver and was described as "imparting tropical fruit" type aromas. The alcohol of **43** is identified in yellow passion fruits.

This thesis the investigation into the kinetics and potential catalysts for the reaction (scheme 18). Both bi-functional (amino-boronic acid) and amine potential catalysts have been screened. Given the preference of enantiopure isomers of **43**, potential catalysts for asymmetric induction have also been studied.

The literature was searched for methods of preparing **43** as a racemate. The method supplied by Oxford Chemicals was a simple solventless addition of thioacetic acid to *trans*-2-Hexenal at 75 ºC.

Three other simple procedures were found for the reaction of thioacetic acid with *trans*-2-hexenal.

1) Addition at low temperature (10 ºC) of the substrates with piperidine as a catalyst followed by stirring at RT for 18 hours [69];

2) Direct addition of the substrates at 0ºC, stirring for 2 hours then warming to room temperature for 24 hours [70];

3) Substrates were heated with benzoyl peroxide at 100 ºC for 3-5 hour[71].

These types of reactions have also been extensively reviewed by Enders [72].

2.2 Preliminary catalyst screening

The reaction of thioacetic acid and *trans*-2-hexenal, scheme 18 (based on the Oxford Chemicals' procedure), was examined using a ^{1}H NMR-based kinetic method, involving following the progress over time. The inherent thermal reaction (neat) is relatively fast, *i.e.* complete in approximately one hour, which could be considered to be sufficiently fast to compete with the required development of a catalytic process. It was therefore necessary to screen for active catalysts which would give much higher rates of reaction to render the background reaction essentially negligible. In order to achieve a sufficiently slow uncatalysed reaction, the reaction was simply diluted to approximately 1 M in D-chloroform under which conditions, the thermal reaction took approximately 3 hours to proceed to 20% completion. Hence, ^{1}H NMR spectra could be accumulated at reasonable time intervals over a period of time (24 hours) by sample removal and dilution to standard NMR concentrations. By comparing the relative integrals of the signal for the CHO group of the product (peaks at δ 9.7ppm) and the signals for the CHO groups in the starting material (δ 9.5 ppm), relative kinetics could be obtained. Thus, a wide range of potential bifunctional organocatalysts **43-49** [73], bifunctional **51** and monofunctional **51, 52** amines as well as phosphines **53** were screened for potential catalytic activity against the reaction shown in scheme 18, using a standard catalyst loading of 10 mol% with all being carried out in D-chloroform. The results for all of these screening reactions are summarised in Figure 4 and Table 1.
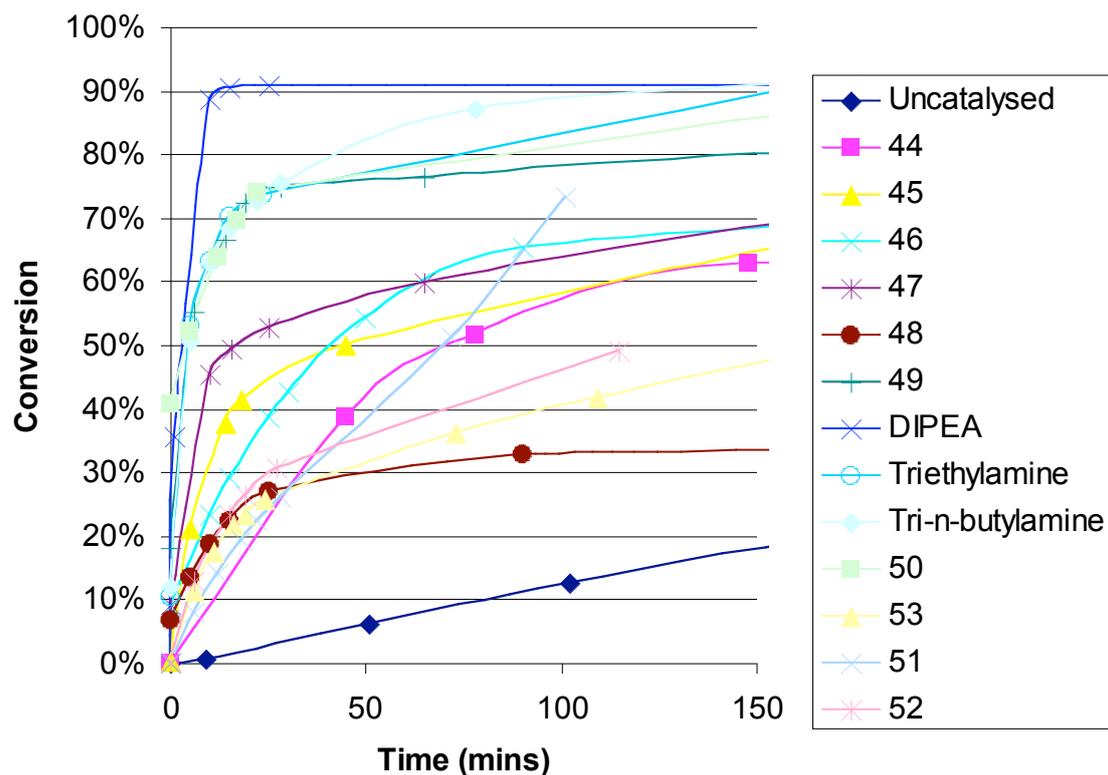
Figure 4 Graph of kinetic data for bifunctional and mono-functional catalysts, in D-chloroform, as listed in Table **1**

Table 1 showing conversions and kinetic results for various catalysts' effects on Equation **1**

Entry	Catalyst	Time (min)	Conversion (%)[a,b]
1	None, Chloroform	300	33

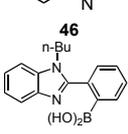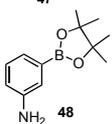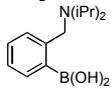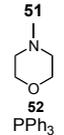|			
2	B(OH)$_2$ / NH$_2$ **44**	300	79
3	N, B(OH)$_2$ **45**	300	77
4	B(OH)$_2$ / N **46**	300	73
5	n-Bu, N, N, (HO)$_2$B **47**	300	75
6	O–B–O, NH$_2$ **48**	300	35
7	N(iPr)$_2$, B(OH)$_2$ **49**	300	80
8	NH$_2$, NH$_2$ **50**	300	100
9	N **51**	300	100
10	N, O **52**	300	59
11	PPh$_3$ **53**	300	64
12	Diisopropylethylamine	300	100
13	Triethylamine	300	96
14	Tributylamine	300	92

a) Determined by ^{1}H NMR. b) extrapolated from kinetic data using Scientis™.

Scientist™ software was used to analyse the data using a first order model.

Initially, (as can be seen from Table 1), catalyst **49** had the most significant rate increase. Catalyst 49 could potentially operate in a bifunctional manner via the boronic acid and tertiary amine groups. However, any bifunctional activity would need to be confirmed by assessing the rate between phenylboronic acid and diisopropylethylamine. Further testing of diisopropylethylamine and phenylboronic acid showed that amine function of the bifunctional catalyst seemed to be responsible for the rate enhancement.

Based on the above results it seemed that an amine based catalyst would be a logical starting point to move towards screening potential asymmetric catalysts. The following amines were screened: triethylamine; tri-n-butylamine; 1,2-diaminecylcohexane, diisopropylethylamine. The rate enhancements were generally poor compared to diisopropylethylamine, which can be seen from Figure 4. A tentative conclusion from this limited study can be drawn: a good catalyst is a tertiary amine, with bulky, electron donating groups; ideally iso-propyl. Therefore a potential asymmetric catalyst could contain this group.

2.2.1 Chiral catalyst synthesis

Attempts to synthesise the iso-propyl derivative of **57** using a variety of reductive amination techniques resulted in failure.

Catalyst **57**[Scheme 19] was therefore synthesised from the free amine by acylation with iso-butyryl chloride, followed by reduction with borane dimethylsulfide complex.
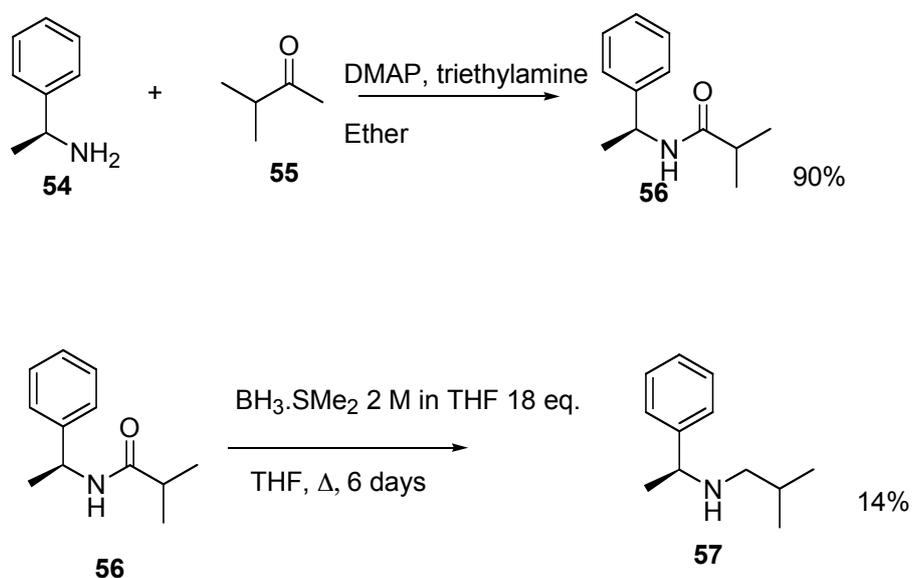
Scheme 19 Synthesis of N-isobutyrylamino catalyst

2.2.2 Screening potential catalysts

A series of chiral catalysts **57-66** (commercially available) were screened under the same reaction conditions and the products of the reactions were analyzed by chiral GCMS. However, no enantiomeric excess was observed in any reactions.
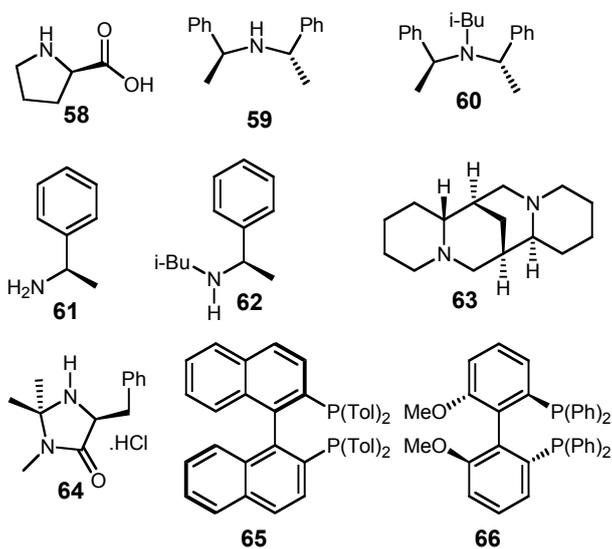
These poor results suggested that the reaction conditions were sub-optimal or simply the catalysts were not associating with the substrates to ensure chiral information transfer.

2.3 Improving the Kinetic Data

Although the NMR kinetic data was useful, the collection method was unreliable (a sample was prepared then taken to the NMR machine as quickly as possible, leading to a potential delay of up to 5 minutes in obtaining spectra, while the reaction was taking place inside the tube). It was felt that the initial few minutes of the reaction was should be more closely studied (which was not possible by the NMR) and another method was sought (which would also provide high accuracy data for the entire reaction).

The issues in particular were attempting to fit the kinetic data; both first and second order models fitted particular examples of the data with no apparent discrimination or logic. Pseudo first order kinetic fitting on the first 10% conversion were not possible due to a lack of data points in the first minutes of the reaction.

The possible quench using methanol (to form the hemi-acetal species) was unsuitable as the reaction was in competition. After addition of methanol it took approximately 10 minutes for the thio-Michael reaction to cease. Another method of kinetic data collection was needed. Chemical engineers routinely use adiabatic calorimetry to probe reactions for safety reasons and for kinetic and thermodynamic data collection. It was decided to use this approach and to obtain extremely reliable and accurate kinetic data.

The approach is extremely simple experimentally. By using adiabatic calorimetry – essentially using a thermometer in a Dewar flask - kinetic and other parameters can be deduced (see equations 9-11).

Prior to any chemical experiments being carried out the thermal properties of the Dewar flask were determined.

The adiabatic assumption is an ideal approximation and as such we must consider:
1. Dynamic errors due to the response of thermometer and mixing rates in vessel are negligible
2. The vessel itself absorbs heat from the reaction mixture during heating.
3. Heat losses as reaction temperature increases.

1 and 2 were determined from simple experiment where hot toluene was added to the flask containing cold toluene and the corresponding temperature transient was monitored. These issues are considered in the following sections.

2.3.1 Dynamics of mixing and temperature probe response

The thermometer response was very fast and the temperature reached a new steady state within 15 seconds. This is considerably faster then the chemical reactions which generally exhibit temperature transients lasting minutes to hours. Errors due to the response of the system were therefore considered to be negligible.

2.3.2 Experimental setup

The experimental setup is simple – a high accuracy digital thermometer linked to a PC, and an extremely cheap Thermos™ flask
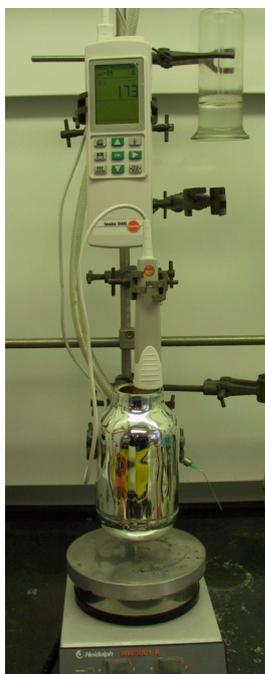

Figure 5 Experimental set-up for adiabatic studies

Thermos flask calibration – mixing solvent of varying temperatures and watching the heat loss curve. This allows ϕ to be calculated. The first time this method was carried out – a liquid nitrogen, expensive, high quality Dewar was used. The thermal capacity of this vessel was large and would have hidden potentially small exotherms. It transpires that the best type of flask for these types of experiment is the cheapest possible, off-the-shelf, commercial flask.

In order to help facilitate data collection a higher boiling point solvent than chloroform was preferred and so toluene was chosen for the reaction solvent for adiabatic calorimetry. (This allowed heat of evaporation losses to be disregarded in the simulation).

Initial examination of the reaction shown in scheme 18 using BatchCAD[72] thermodynamic property estimations suggested that it should be significantly exothermic with an estimated heat of reaction of -5.2×10^4 kJKg^{-1}mol^{-1}. In order to confirm these calculations and quickly screen for reaction rates under a series of different conditions, a simple Dewar flask was used as a reaction vessel and the subsequent adiabatic temperature profiles recorded.
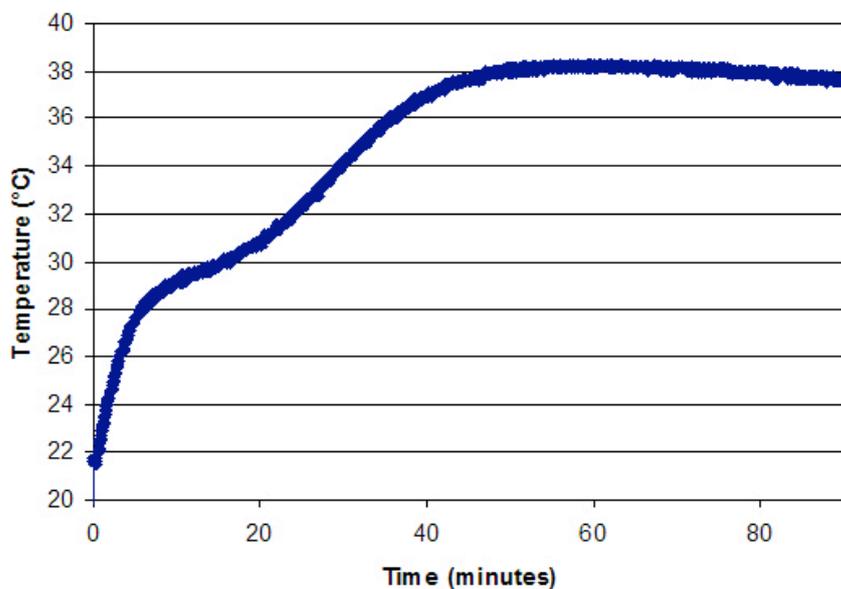
2.4 Results from thermo-chemistry

Figure 6 Initial temperature vs time plot from digital thermometer, batch addition of thioacetic acid, *trans*-2-hexenal in toluene

Figure 6 shows a two stage exothermic reaction with approximately half the energy of the reaction in each stage.

The two stage exotherm seen requires the formation of a stable intermediate which then slowly forms the product.

The traditional Michael mechanism under acid catalysis is a protonation of the aldehyde, attack of the nucleophile on the remote alkenic carbon, followed by a keto-enol tautomerisation to yield the final product.

In order to test the heat output, a reaction substituting acetic acid for the thioacetic acid was carried out and showed no exotherm. It was therefore reasonable to assume that the protonation of the aldehyde was not responsible for the first exotherm.

Keto-enol tautomerisations are considered to be fast and under the reaction conditions it was not considered reasonable that the enol form of the product would be long lived.

35

Based on this we discounted the Michael addition mechanism as a reasonable explanation for the two-stage exotherm which was observed.

A new mechanistic explanation was sought to explain the two-stage exotherm. This mechanism had to have a stable intermediate.

It was postulated that an initial 1,2 addition to the carbonyl followed by a 3,3 rearrangement could explain the two-stage exotherm.
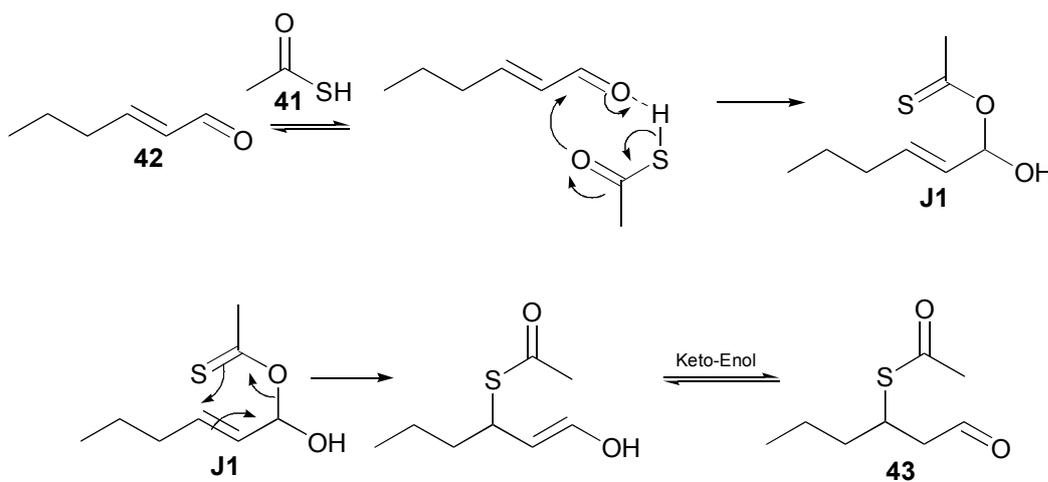
Scheme 20 – proposed mechanism

These types of hemi-thioacetal intermediates are known to undergo rearrangements [73]:
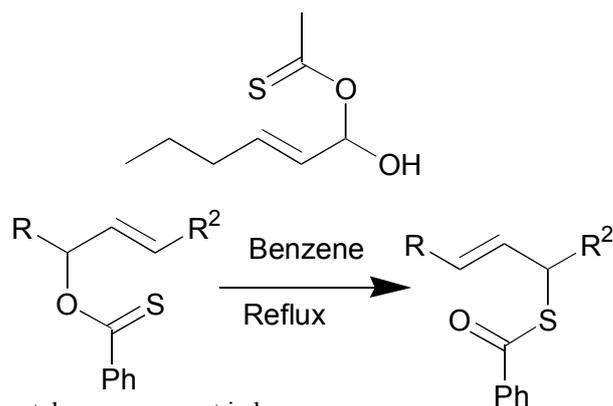
Scheme 21 hemi-thioacetal rearrangement in benzene

2.5 Low temperature experiment

It was thought that by lowering the temperature of the reaction we might be able to "trap" the intermediate and analyse its structure.

An adiabatic temperature rise normally exhibits self-acceleration due to positive feedback of temperature with Arrhenius kinetics. The presence of a distinct second adiabatic temperature rise is usually caused by the primary reaction raising the system temperature to a sufficient level that a secondary reaction is initiated.

In all the above experiments there was a small deviation from ideal adiabatic reactor behaviour due to heat loss, with gradual cooling of the system as the reaction goes to completion. As a result of this cooling, the temperature derivative, dT/dt, may be reduced between the first and second transients (Figure 8) and, as shown, with higher heat loss the derivative may tend to zero or even become negative.

This is an important observation: if $dT/dt \leq 0$, positive feedback of temperature to produce self-acceleration cannot occur. The second temperature rise is, therefore, not an onset Arrhenius effect. This self-accelerating reaction must be due to the inherent reaction mechanism being in some way autocatalytic.
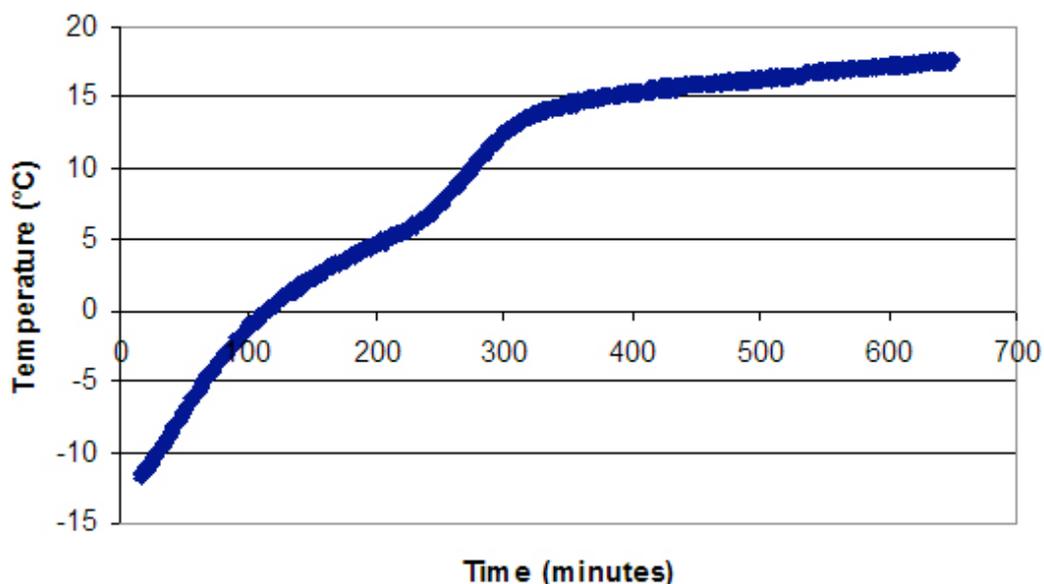
Figure 7 – low temperature experiment

When an experiment was conducted with an initial temperature of −12 °C the same dual temperature phase behaviour was observed, with the second phase now commencing at 5 °C, rather than 28 °C. The time period of the initial phase was approximately 150 minutes (Figure 7) and the second temperature rise lasted for about 60 minutes.

These times contrast with those in Figure 6 where the first temperature rise took about 8 minutes and the second 30 minutes. The first reaction is significantly accelerated at a higher operating temperature and conforms to Arrhenius behaviour whereas the second reaction is not significantly accelerated thus supporting the suggestion of chemical self-acceleration. Whether there is an intermolecular or intramolecular contribution could be determined by an Eyring plot to determine the magnitude of the entropy contribution to the free energy.
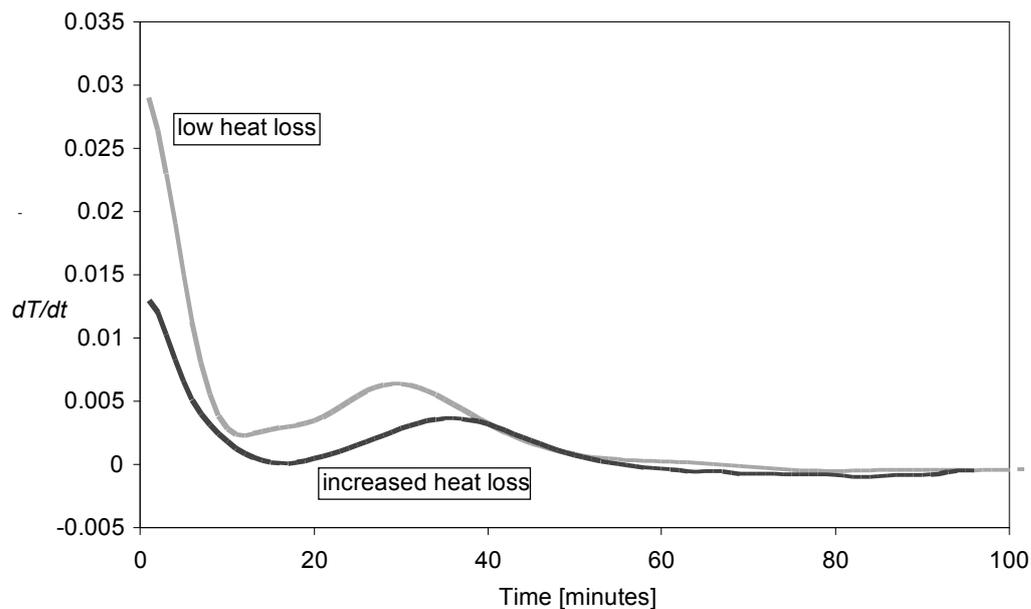
Figure 8 – High and low heat loss experiments for scheme 18 in toluene (thanks to Prof AR Wright for derivative calculations)

2.6 Development of a kinetic model

The approach adopted used a combination of chemical knowledge with the reaction modelling method described above. A reaction network is a prerequisite for the regression of kinetic parameters and the use of process modelling and simulation tools. Normally, a network is derived from a proposed reaction mechanism. In this work the process is reversed. First, a reaction network is resolved heuristically such that kinetics parameters can be regressed to the observed adiabatic temperature profiles for all solvent systems. This network, together with the associated rate constants, was then used to derive a chemical reaction mechanism. The network is summarised in Table 2.

39

For the bimolecular addition reaction between A and B to give J1 the rate expression for the forward step is: $k_1[A][B]$

For the reaction of J1 to give A and B (the backward reaction) the rate expression is: $k_2[J_1]$

The reaction of J1 to give the product P has a rate expression consisting of two terms, the collapse of the intermediate: $k_3[J_1]$ and the production of the product through hthe auocatalytic step: $k_4[J_1][P]$

Table 2. Reaction network for thioacetic acid **41** with *trans*-2-hexenal **42** and the reaction enthalpies used in the regression.

Entry	Reaction	Rate expression	ΔH (kJ kmol^{-1})
1	$A + B \rightarrow J_1$	$k_1[A][B]$	-5.2×10^4
2	$J_1 \rightarrow A + B$	$k_2[J_1]$	5.2×10^4
3	$J_1 \rightarrow P$	$(k_3[J_1] + k_4[J_1][P])$	0

Where A is thioacetic acid **41**; B is *trans*-2-hexenal **42**; J_1 is an intermediate; and P is the product, 3-acetylthiohexanal **43**. It should be noted that in chemical engineering all rate expressions are positive, the reaction order provides the 'direction'.

In the above model (Table 2), equilibrium is established between the first and second reactions (entries 1 and 2, respectively), with a resulting exotherm which produces the first temperature rise. The second temperature rise is due to a shift in the position of this equilibrium by the autocatalytic transition from intermediate J_1 to product **43**, *i.e.* a third reaction occurs, as represented by entry 3 (Table 2). An overall heat of reaction was calculated from the adiabatic temperature increase in the toluene experiments with a correction for Q_{loss} and ϕ. In the above scheme this enthalpy has been assigned to the formation of the intermediate J_1: although this is thermodynamically unlikely, little improvement to kinetic fitting was achieved by assigning an enthalpy to the third step of the reaction at the expense of the first step.
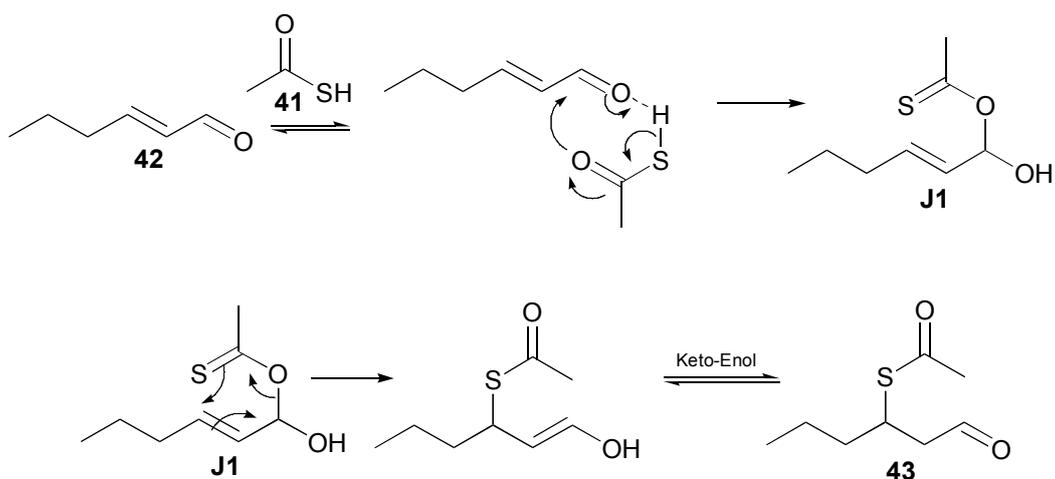
Scheme 20 – proposed mechanism (repeated for clarity)
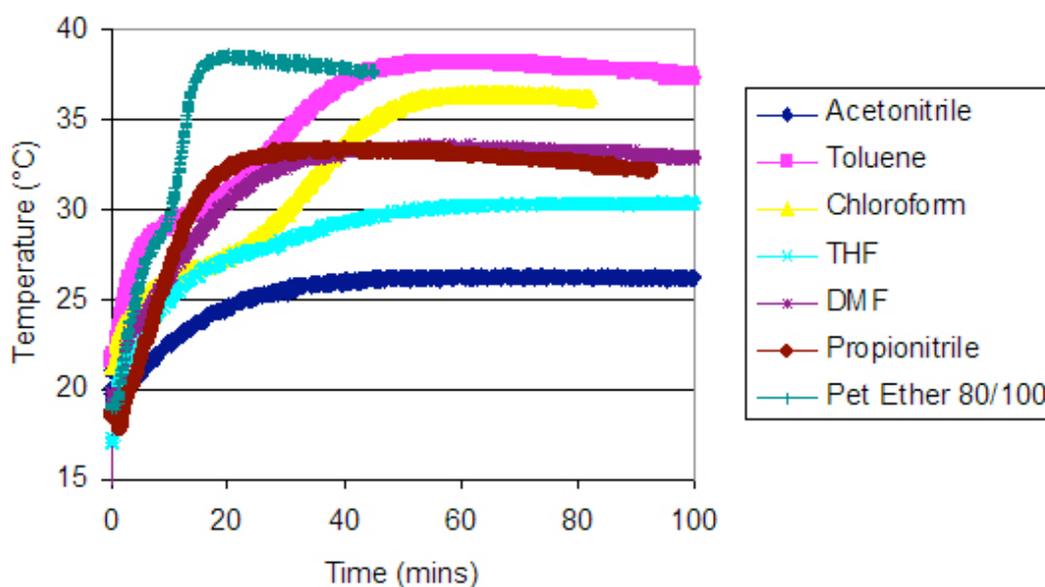
Figure 9 – Solvent screening for scheme 18, individual plots as well as derivatives are shown in Figure 10

Isothermal rate constants were regressed to the recorded temperature profiles for each solvent using the kinetic fitting facility of BatchCAD and the results are shown in Table 2. Although reactions 1 and 2 in Table 2 are temperature dependent, the model uses an isothermal approximation (as the model incorporates an autocatalytic step Arrehnius

41

fitting is no longer appropriate). The primary focus was to resolve the network and the added detail of temperature varying rate constants for entries 1 and 2 was unwarranted. (It perhaps should be noted that throughout this work where BatchCad is used to provide data the units are often unusual as BatchCad is primarily used for industrial chemistry which has different requirements).

Table 3. Rate constants for the reaction of thioacetic acid **42** with *trans*-2-hexenal **41**. The superscript n defines the order fo the reaction so the correct units can be deduced for the rate constant

| Entry	$(m^3kmol^{-1})^{n-1}$ s^{-1}	Toluene	Chloroform	DMF	THF	MeCN	EtCN	Pet. ether
1	k_1	3.5×10^{-3}	1.6×10^{-3}	1.1×10^{-3}	9.7×10^{-4}	6.2×10^{-4}	3.8×10^{-3}	5.5×10^{-3}
2	k_2	2.5×10^{-3}	5.2×10^{-4}	2.2×10^{-4}	1.9×10^{-4}	4.4×10^{-4}	1.5×10^{-2}	8.2×10^{-2}
3	k_3	3.6×10^{-5}	3.4×10^{-3}	1.5×10^{-2}	3.1×10^{-4}	1.5×10^{-7}	4.1×10^{-5}	2.2×10^{-7}
4	k_4	1.5×10^{-2}	3.7×10^{-2}	$<1 \times 10^{-5}$	$<1 \times 10^{-5}$	$<1 \times 10^{-5}$	0.36	0.14

Figures 10a-n show the measured adiabatic temperature profiles for each of the solvent systems and the profiles simulated using the rate constants from Table 3. In all cases there is a close match. The corresponding simulated composition profiles for each of the solvent systems are shown in Figures 10a-n. The minor differences in peak temperatures achieved for the various solvents are due to the differences in specific heat capacities and accumulated heat losses. The similarly minor differences in the shapes of the temperature transients are due to the differences in the reaction rate constants affecting the reaction network dynamics. The acetonitrile system is anomalous as it forms the intermediate J_1 but does not react further. An NMR study was undertaken and showed no formation of product even after 8 hours.

a

b

c

d

e

f

g

h

i

j

k

l

m   **n**
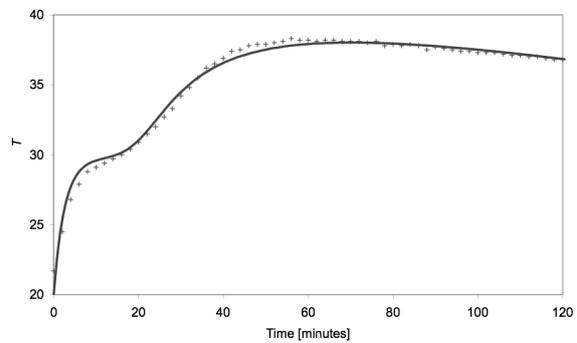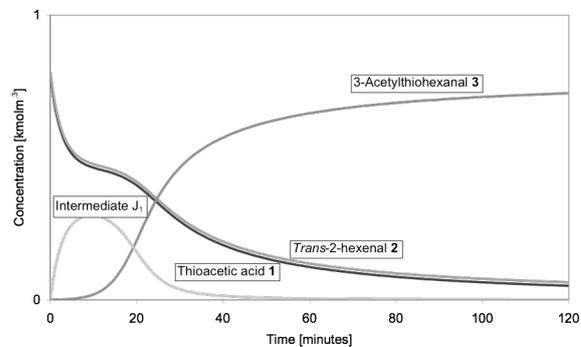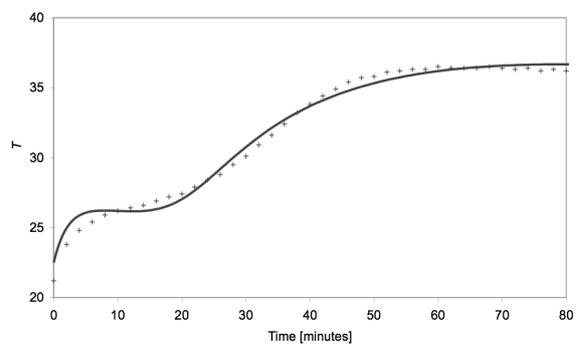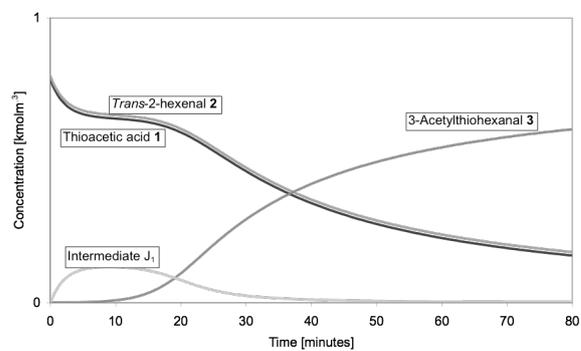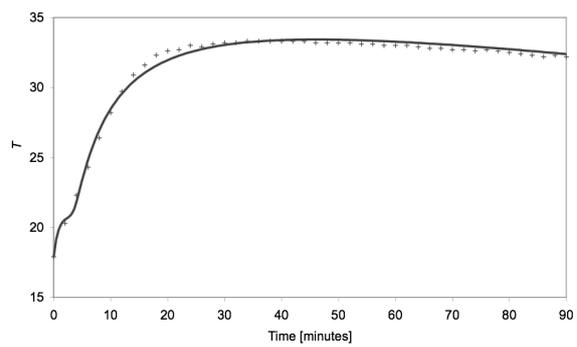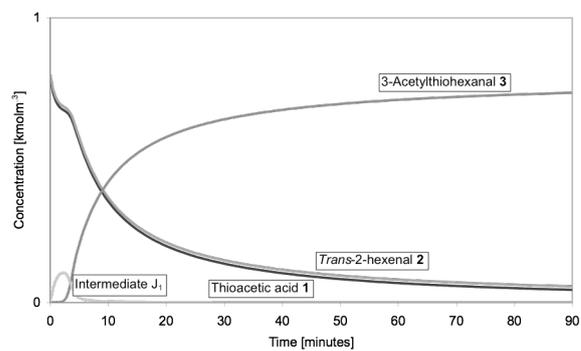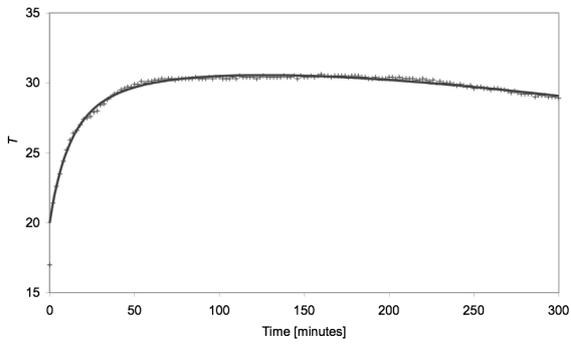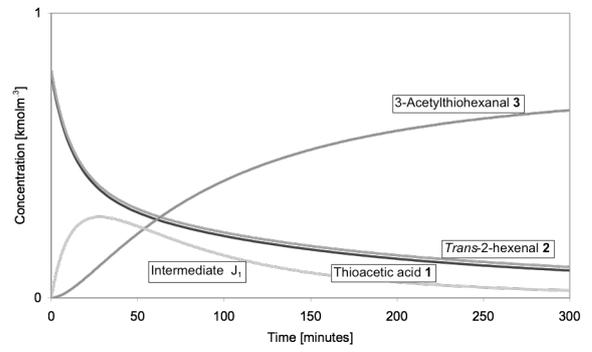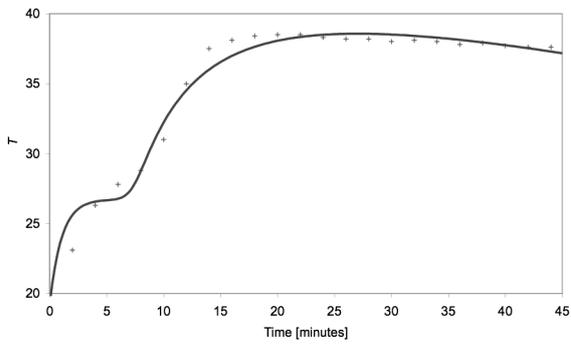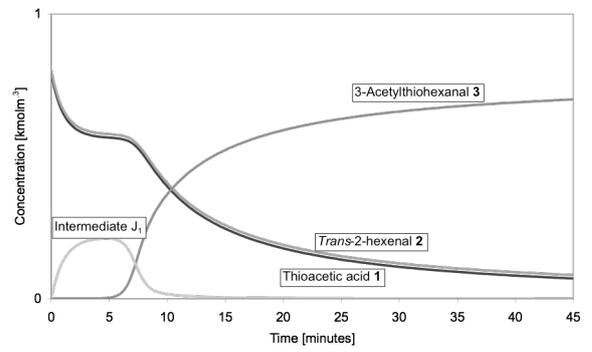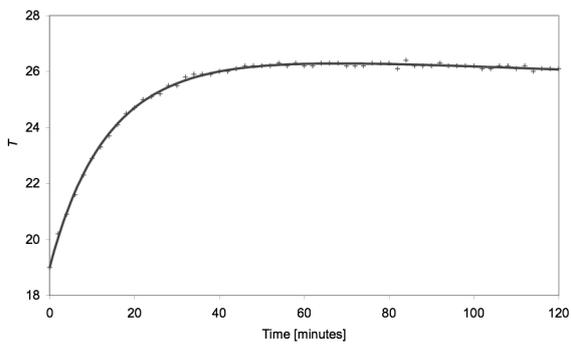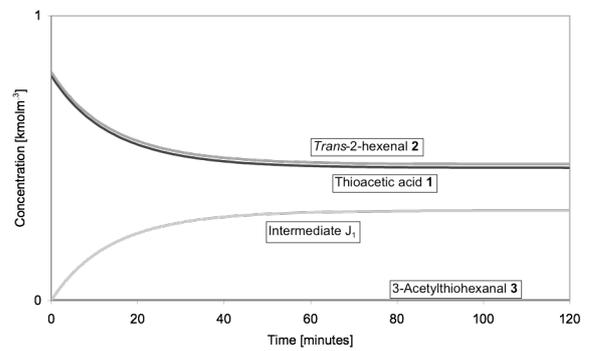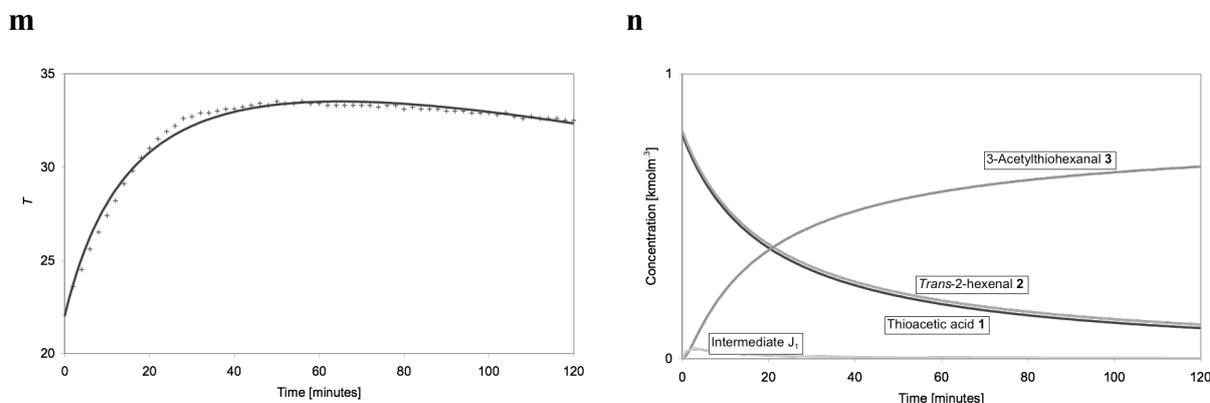
Figure 10. Actual and simulated temperature profiles, and predicted composition profiles for reaction of thioacetic acid **42** with *trans*-2-hexenal **41**. **a**; Actual and simulated temperature profile in toluene. **b**; Predicted composition profile in toluene. **c**; Actual and simulated temperature profile in chloroform. **d**; Predicted composition profile in chloroform. **e**; Actual and simulated temperature profile in propionitrile. **f**; Predicted composition profile in propionitrile. **g**; Actual and simulated temperature profile in THF. **h**; Predicted composition profile in THF. **i**; Actual and simulated temperature profile in petroleum ether. **j**; Predicted composition profile in petroleum ether. **k**; Actual and simulated temperature profile in acetonitrile. **l**; Predicted composition profile in acetonitrile. **m**; Actual and simulated temperature profile in DMF. **n**; Predicted composition profile in DMF.

Figures 10 a, i and m have a poor fit compared to the other profiles. As such some caution must be taken in the interpretation

§ 2.8, table 4 provides an NMR discussion on these results

Thanks to Prof AR Wright for the kinetic fitting using BatchCad and providing derivative graphs

For the solvents toluene, chloroform, propionitrile and petroleum ether, the intermediate J_1 is quickly formed, however, there is a significant autocatalytic rate (k_3 and k_4) which results in its rapid consumption. This effect results in the characteristic sigmoidal shape of the temperature transients for these solvents and is further illustrated by the simulated composition profiles predicted by the model. In the case of DMF, the autocatalytic rate k_4 tends to zero, however, the transformation of the intermediate J_1 to product **3** is very

rapid due to the relatively high value of k_3. The rate limiting step is entry 1 and, therefore, no sigmoidal shape appears in the temperature transient. THF shows a similar effect, however, k_3 is significantly less than for DMF and the simulation predicts that the intermediate J_1 will decay slowly. Finally, for acetonitrile, both k_3 and k_4 tend to zero which would produce about 40% conversion of the thioacetic acid **42** and *trans*-2-hexenal **41** to the intermediate J_1 and no further reaction by NMR (monitored over 16 hours).

2.7 Reaction Probing using React-IR

In an attempt to further understand the reaction and its clearly complex mechanism, React-IR studies were carried out (switching from toluene to chloroform for easier analysis).
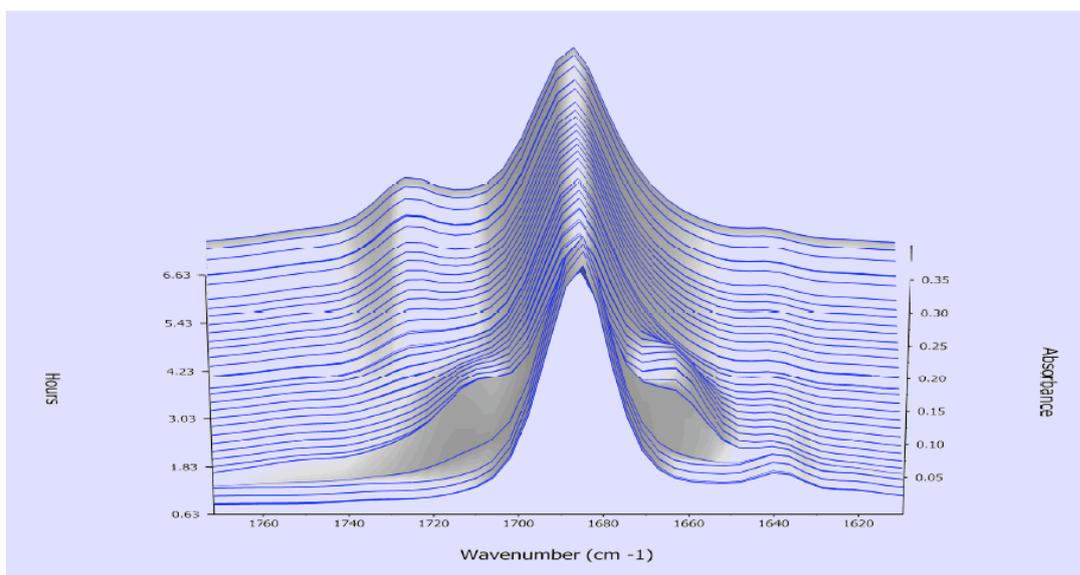
Figure 11 - ReactIR spectrum for the reaction *trans*-2-hexenal with thioacetic acid (added after 1 hour) in chloroform.

As can be seen at 1662 cm^{-1} there is a rapid formation of an intermediate. Resulting component analysis shows evidence for all the starting material, the intermediate build up and tail off (figure 12). It also tentatively suggests the formation of a second intermediate or compound which is as yet not understood. Although this reaction was not carried out in a Dewar flask (and hence under pseudo-isothermal conditions), the intermediate

46

formation and product formation are at a time stamp comparable to the adiabatic experiments.
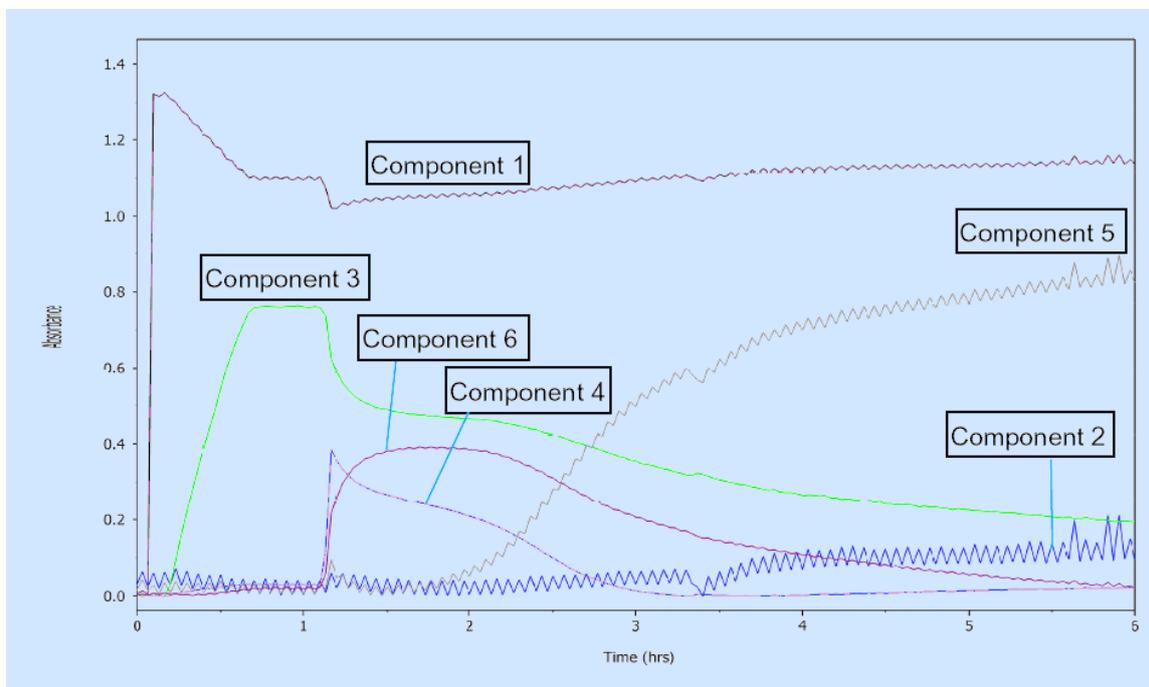
Figure 12 - Component analysis suggesting that six species are present including chloroform. Colour key: Red = Component 1 (chloroform); Blue = Component 2 (intermediate J_2); Green = Component 3 (*trans*-2-henenal); Pink = Component 4 (thioacetic acid); Grey = Component 5 (3-acetylthiohexanal); Purple = Component 6 (intermediate J_1).

2.8 Reaction Probing using NMR

In a further attempt to understand the structure and hence mechanism a detailed 1H NMR spectroscopy study was carried out. Initially the study was carried out using *trans*-2-hexenal however the complexity of the methyl region prevented full characterisation of the structures. However, using this study as a starting point, switching to crotonaldehyde as the substrate simplified the methyl region of the spectrum. Thermochemical studies showed that the crotonaldehyde reacted producing the same sigmoidal shape of temperature versus time graph. [The second 1H NMR study was carried out by G. Illyashenko as I was incapacitated by a serious long term illness and thanks are offered to him for his assistance during that difficult time].

Table 4. ^{1}H NMR spectrum assignments associated with the thioacetic acid **42** crotonaldehyde **67** reaction (Spectra collected in d_8-toluene for best resolution on a Bruker 400 MHz NMR spectrometer with exception of Intermediate J_2, which was collected on a 500 MHz Bruker NMR spectrometer; δ is reported in ppm referenced to CH_2Cl_2).

Entry	Structure	Assignment	Notes
1	Starting material **67** 	δ 1.42 (3H, dd, J = 6.8, 1.6, Me), 5.80 (1H, ddq, J = 7.6, 15.6, 1.6 Hz, H(b)), 6.09 (1H, dq, J = 15.6, 6.8 Hz, H(c)), 9.20 (1H, d, J = 7.6 Hz, H(a))	
2	Product 	δ 1.30 (3H, d, J = 7.2 Hz, Me(a)), 2.25 (3H, s, Me(b)), 2.58 – 2.72 (2H, m, H(b)), 3.80 – 3.98 (1H, m, H(c)), 9.64 (1H, t, J = 1.8 Hz, H(a))	
3	Intermediate J_1 (**68**) 	δ 1.14 (3H, d, J = 7.2 Hz, Me(a)), 1.84 (3H, s, Me(b)), 4.19 (1H, dd, J = 10.0, 6.4 Hz, H(b)), 4.37 (1H, dq, J = 10.0, 7.2 Hz, H(c)), 6.14 (1H, t broad, J = 6.4 Hz H(a)), 7.45 (1H, s, broad H(d))	J(ac) is small for the *trans*-coupling, however, the *trans*-arrangement was established through NOE; signal at 6.14 ppm resolves to doublet in MeCN upon shake with D_2O with J = 6.4 Hz; signal at 7.45 is exchangeable proton
4	Intermediate J_2 (**69**) 	δ 1.21 (3H, d, J = 6.8 Hz, Me(a)), 1.80-1.85 and 1.94-2.02 (2H, m + m, H(b)), 3.76 – 3.88 (1H, m, H(c)), 5.72 (1H, dd, J = 9.5 Hz (*anti*), J = 4.0 Hz (*syn*), H(a))	This is a mixture of diastereoisomers (1:1), data is reported for only one; signals corresponding to Me(c + b) are masked by other signals; H(a) and H(c) both couple to signals assigned to H(b), which was established through COSY NMR; H(b) signal is very complex and further masked by other Me groups.
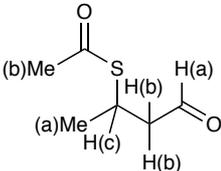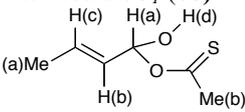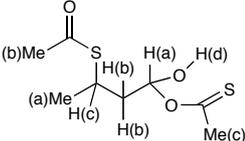
The NMR results show strong supporting evidence for the postulated thiohemi-acetal intermediate J_1 shown in scheme 20. The second "intermediate" J_2 has yet to be confirmed in any reaction network or role in the overall synthetic scheme. This work is continuing.

2.9 Investigation of other substrates

The project, so far by using two simple unsaturated aldehydes, has determined that a hitherto unknown reaction mechanism is operating.

So far in this study it has been shown that thioacetic acid reacts in an unusual manner with unsaturated aldehydes. To complete this study further investigation into other sulfur nucleophiles and other unsaturated carbonyl systems was needed. After initial synthesis of the expected product, a quick investigation of the thermochemical and React-IR spectra would show any unusual activity during the reaction.

The rationale to select other substrates was

1) Availability (time was running out on this project so "off the shelf" materials were needed)

2) a series of unsaturated compounds with differing functionality: esters, aldehydes, nitro-alkenes

3) other sulfur nucelophiles to determine if the thioacid moiety was necessary (and would subsequently provide support for the postulated scheme 20)

2.9.1 Synthesis of relevant products for mechanistic investigations

It should be noted for clarity that acetonitrile was not considered suitable for a solvent due to the stalling of the reaction, discussed at the end of section 2.6. Where acetonitrile would have been used propionitrile was substituted.

Product **71** was successfully synthesised in 62% yield according to scheme 22.

49
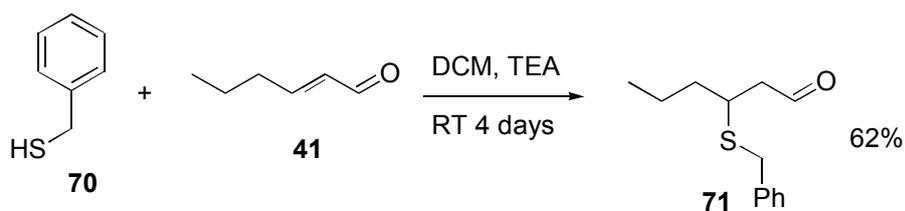
Scheme 22

Product **73** was successfully synthesised in 84% yield according to scheme 23.
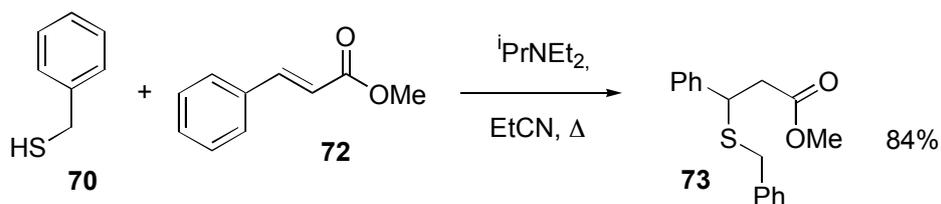
Scheme 23

Product **75** was successfully synthesised in 88% yield according to scheme 24.
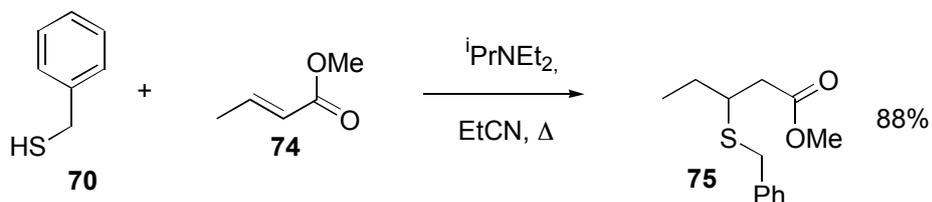
Scheme 24

Product **77** was successfully synthesised in 63% yield according to scheme 25.
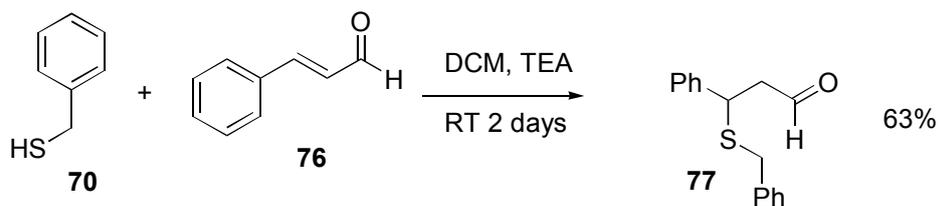
Scheme 25

Product **79** was successfully synthesised in 78% yield according to scheme 26.
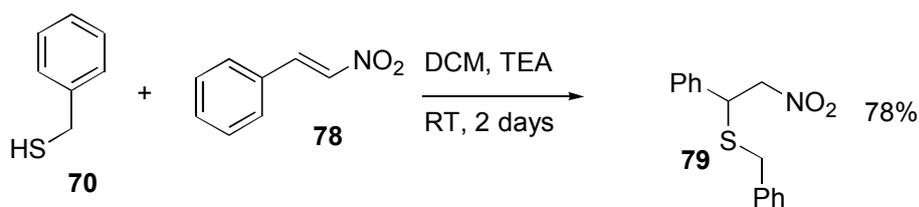
Scheme 26

Product **80** was successfully synthesised in 44% yield according to scheme 27, however material degrades under silica gel chromatography conditions and therefore, difficult to obtain high yields.

Scheme 27

Attempted synthesis of **82**, has proved difficult (scheme 29).
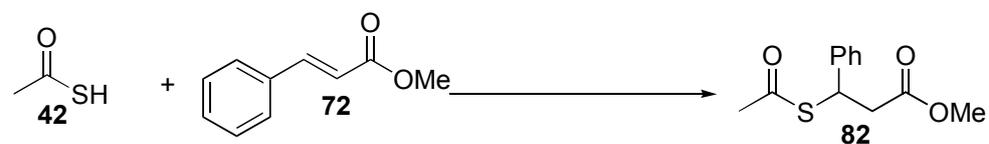
Scheme 29

Refluxing in proprionitrile using Hünig's base as a catalysis showed complete conversion by TLC, however, no product was observed after work up and column chromatography. The product was presumably decomposing at some point during the purification process. A further reaction was carried out and when the reaction appeared to be complete by TLC, the reaction was worked up. TLC comparisons reveal that the work up process eliminated the thioacetic acid to give starting material **82**. Before this uncatalysed reaction could be studied this material would need to be reduced in-situ for characterisation and yield determination. The project finished before this could be completed.

Product **71** was successfully synthesised in 66% yield according to scheme 30.
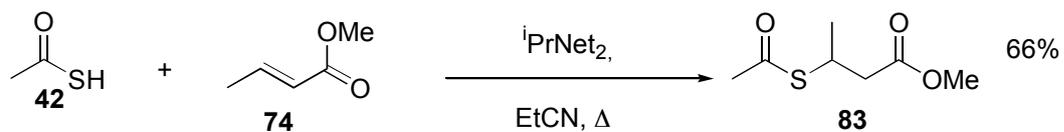
Scheme 30

Product **71** was successfully synthesised in 72% yield according to scheme 31.
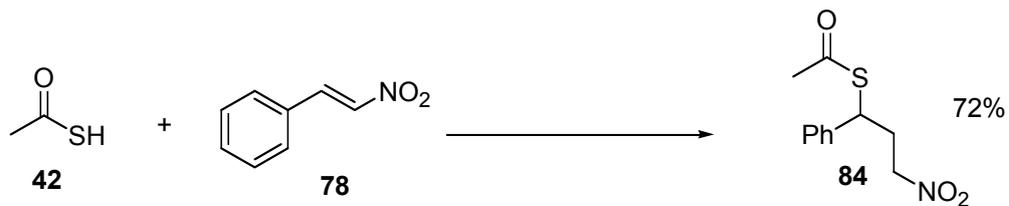
Scheme 31

2.9.2 Thermochemical and React IR investigations

Once the products of the previous reactions had been synthesised, the uncatalysed reaction could be studied to see whether these systems would produce similar sigmoidal graphs and React-IR profiles compared to section 2.4

Table 5 S-H additions for various substrates, 1 M solution in toluene

| Entry	Nucleophile	Electrophile	Thermochemistry	React-IR
1	**42** (acetyl-SH)	**76** (Ph-CH=CH-CHO)	Sigmoidal shape	Multi-component
2	**42** (acetyl-SH)	**74** (crotonate OMe ester)	No exotherm	No reaction
3	**42** (acetyl-SH)	**78** (Ph-CH=CH-NO₂)	Sigmoidal shape	Multi-component
4	**42** (acetyl-SH)	**72** (Ph-CH=CH-CO₂Me)	Sigmoidal shape	Multi-component
5	**70** (Ph-CH₂-SH)	**41** (enal)	No exotherm	Some product, no intermediate observed
6	**70** (Ph-CH₂-SH)	**67** (crotonaldehyde)	No exotherm	No obvious reaction
7	**70** (Ph-CH₂-SH)	**76** (Ph-CH=CH-CHO)	No exotherm	Some product, no intermediate observed
8	**70** (Ph-CH₂-SH)	**78** (Ph-CH=CH-NO₂)	No exotherm	No reaction
9	**70** (Ph-CH₂-SH)	**72** (Ph-CH=CH-CO₂Me)	No exotherm	No reaction

53

Entries 1,3 and 4 in table 5 show sigmoidal shapes in the thermochemistry and multicomponents in the React-IR analysis.

Unfortunately this project ended before further investigation of entries 1,3 and 4 could take place. Future work should consist of NMR investigation and thermochemical data fitting in BatchCad to determine if the reaction network proposed in Table 2 correspond.

2.10.0 Investigation of potential Amine-based catalysts

Having discovered a new mechanism for the addition of thioacetic acid **1**, to certain unsaturated carbonyl systems as well as ester and nitro-ene systems, the question of how amine catalysts behave is still open to question. Under our present scheme (§2.4, Scheme 20) the mechanism relies heavily on hydrogen bonding. If the capability for hydrogen bonding is removed, by ensuring the thioacetic acid is in its de-protonated form, then how this system behaves thermochemically could be extremely interesting.

In order to investigate this it was decided to return to the thioacetic acid **1** addition to hexenal **5**, by adding 100 mol% Hünig's base to thioacetic acid, followed by hexenal.

The results are surprising.
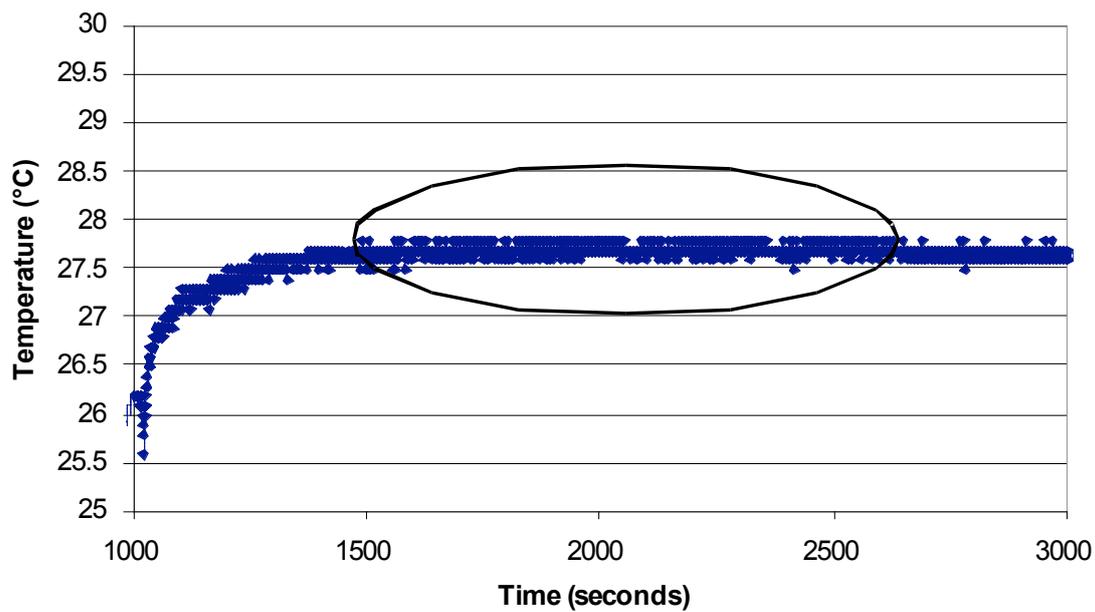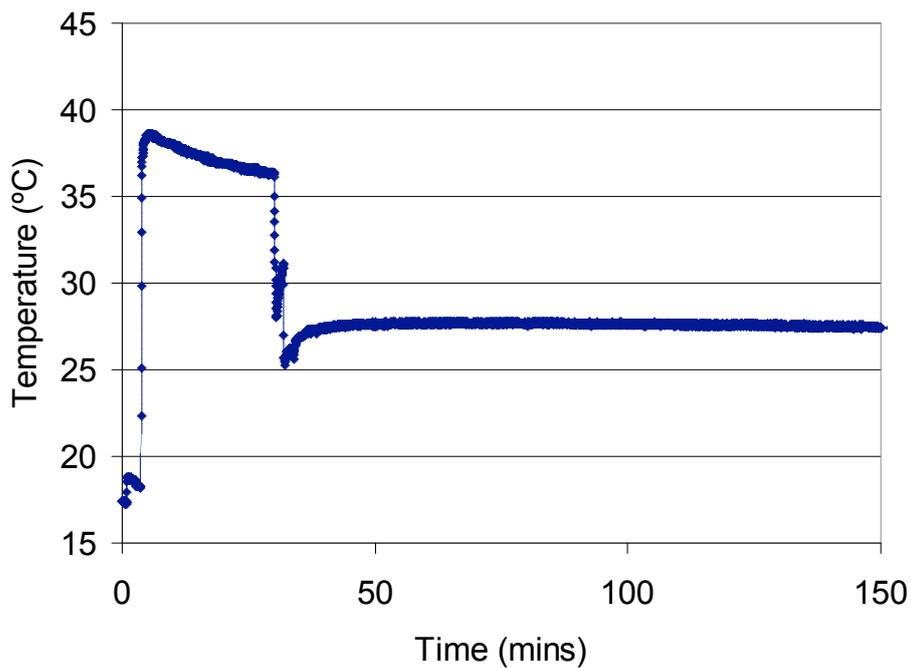
Figure 13 Investigation of effect of amine catalysis, with expansion to show plateau

As can be seen the initial heat of neutralisation is very exothermic, the contents of the flask was then cooled to approximately 25 °C, after addition of hexenal (33 minutes) the

reaction exotherms, plateaus, then cools down. This sigmoidal shape indicates a two stage process occurring.

Further investigation of this, including the reverse addition, NMR and react-IR is needed, however, this project ended before this work could be completed. Should further work show that the mechanism postulated in scheme 20 applies to a catalysed system, it would help to explain why no enantioselectivity was shown during the chiral catalyst screening.

2.11 DMSO Solvent Screen

During the solvent screening for the reaction of thioacetic acid and *trans*-2-hexenal an unusual side reaction was noticed when DMSO was used. Elemental sulfur was precipitated from the reaction medium. Further investigation of this system was needed to determine the origin of the elemental sulfur and what reaction, if any, had occurred to the thioacetic acid and hexenal.

The first series of reactions were carried out as scoping reactions:

- Hexenal, thioacetic acid and DMSO produced elemental sulfur
- Thioacetic acid and DMSO produce sulfur.

NMR studies showed that the hexenal was not consumed. In the reaction of thioacetic acid and DMSO elemental sulfur was produced.

When the reaction was carried out in deutero-chloroform there were ^{13}C peaks suggesting diemthylsulfide formation.

The reaction was monitored in chloroform and toluene on the React IR system:

DMSO and thioacid
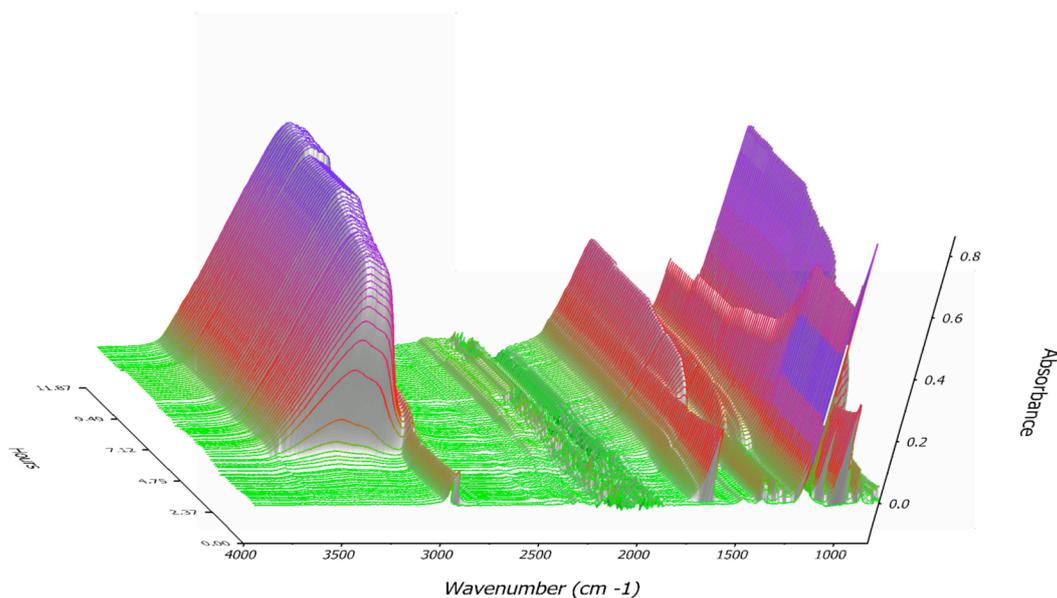
Figure 14 – reaction in chloroform

As can be seen in figure 14, there was a build up of water or ROH species. There was a 3 hour delay before the peaks at 3500 cm^{-1} started to appear, in toluene this peak formation is *immediate*.

It was also noticed that the mixture became bi-phasic under these conditions.

The reaction of thioacetic acid and DMSO was HIGHLY exothermic – a mixture of 20mL of both reactants (React IR scale) results in an exotherm from 20 ºC to 98 ºC in 6 seconds. This corresponds to approx 1600 J or 266 W. What is also noticed is that the mixture continued to bubble as the reaction cooled down. Bubbling stopped at 69 ºC. Of the starting materials thioacetic acid boils at 98 ºC and DMSO at a much higher temperature. The continued presence of bubbling suggests a gas or highly volatile chemical is produced. This would correspond with dimethylsulfide production. It was also noted that this refluxing reaction takes much longer to form sulfur than when it does not reflux (which may suggest some sort of solubility effect). The volatile liquid/gas was collected by a cold finger and was diemthylsulfide by olfactory and NMR evidence.

Approximately 20 mol% Sulfur is produced relative to thioacetic acid for these reactions

Further GC-MS data show m/z ions for S_8 and DMS together with ions at m/z 151 and 183, which could be diacetyl-di- and tri- sulfides (Figure 15) or a substance with a similar formula. These observations may well shed some light on the mechanism of the process.

1 n = 2 or 3
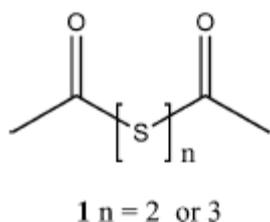
Figure 15 – possible structures

2.12.0 Conclusions

We have tested a wide range of potential catalysts for the reaction of thioacetic acid and *trans*-2-hexenal and the rate data observed. Alkyl amines give excellent rate enhancement for this reaction, however they do not perform as asymmetric catalysts. In the course of searching for chiral induction we have yet to see any evidence for this and regard the inherent thermal background reaction as a major problem in this search.

In a search for better kinetic data we used a combined, multi-disciplinary chemistry-chemical engineering approach towards mechanism determination which has proven to be a powerful method for reaction investigation. Using this approach, we have elucidated a new mechanism for thioacetic acid additions to unsaturated aldehydes which is not

related to the process which is normally associated with thio-Michael-additions and is likely to have repercussions upon asymmetric additions. The reaction network derived by kinetic modelling from adiabatic calorimetry provides a single mathematical framework from which kinetic parameters may be regressed. Each of the solvents affects the magnitudes of the rate constants of the network in different ways with a result that the recorded temperature profiles display a variety of shapes. There is good correlation between the NMR and thermal data, which leads to the confirmation of a new reaction network, involving one or more intermediates and competitive reaction processes. From this, the mechanism we propose is a new, self-accelerating process, in which the product may catalyse collapse of one observable intermediate to the product. The exact mode of this autocatalytic step is not clear at present, but is the subject of ongoing studies as is the generality of this new mechanistic insight into the Michael addition reaction.

3.0 Experimental

General section

All ^{1}H and ^{13}C NMR were recorded with either a Varian Mercury-400, Bruker Avance-400 or Varian Inova-500 spectrometers. Chemical shifts are expressed as parts per million (ppm) downfield from the internal standard TMS. Mass spectra were recorded using a Thermo Finnigan LTQ FT mass spectrometer. IR spectra were recorded with a Perkin–Elmer 1615 FTIR spectrometer. Elemental analysis was performed using an Exeter Analytical E-440 Elemental Analyser. Melting points were determined using an electrothermal melting point apparatus. All reagents were obtained from Aldrich or Lancaster and were used as received. Reactions were stirred using a magnetic stirrer bar.

Reactions after work up were dried using anhydrous magnesium sulfate and all evaporations were carried out using Büchi rotary evaporator *in vacuo* (*ca.* 15 mmHg), followed by drying under high vacuum (*ca.* 0.2 mmHg).

ReactIR studies

Standard Operating Procedures for a Mettler-Toledo React-IR 4000 were employed using ReactIR v3.1.0.0 and ConcIRT AF v3.5.0.4 software. A background spectrum of air was taken first. The reaction sequence employed 128 sweeps per scan and 1 scan per minute. All experiments employed the following general sequence: 1) the probe was immersed in the vessel of solvent; 2) the reaction collection was started; 3) a baseline was established; 4) the first reagent was added; 5) the baseline was re-established; 6) further additions of reagents were followed by baseline re-establishment as appropriate.

General procedure for the addition reactions carried out in the Thermos flask

All adiabatic reactions were carried out using a Thermos Model 32-34-50 flask, Filler 32-50F with a 0.5 L capacity, equipped with magnetic stirring. All temperature readings were made using a Testo 946 digital thermometer with a Testo Type T temperature probe linked to a PC via an RS232/USB connector. Data was stored directly on the PC using the Testo Comfort software and exported to MS Excel for data processing. The Dewar flask, fitted with its temperature probe was closed with a cotton wool plug to reduce evaporative heat loss.

General Synthesis of 3-acetylthiohexenal (43)

A mixture of chloroform (15 mL), and *trans*-2-hexenal (1.64 mL, 0.014 moles) was treated with thioacetic acid (1 mL, 0.014 moles). After 12 hours, the mixture was evaporated and purified by silica gel chromatography (100% DCM eluant); yield 2.2 g, 90%, spectra correspond to known data [74];

Synthesis of 3-acetylthiohexenal (43) – kinetic experiments

A mixture of deutro-chloroform, catalyst (10 moles %) and *trans*-2-hexenal was treated with thioacetic acid and the reaction was monitored by removing aliquots (0.3 mL)

removed from the flask which were diluted in an NMR tube. See table 6 below for further details of quantities.

Table 6

Entry	Catalyst	Moles	Mass (g)	Vol (mL)	Thioacetic acid Moles	Vol (mL)	*trans*-2-hexenal Moles	Vol (mL)	CDCl₃ Vol (mL)
1	none				0.014	1	0.014	1.64	neat
2	none				0.014	1	0.014	1.64	15
3	(3-aminophenyl)boronic acid **44**	0.00046	0.072		0.0047	0.33	0.0047	0.55	5
4	quinolin-8-ylboronic acid **45**	0.00046	0.080		0.0047	0.33	0.0047	0.55	5
5	quinolin-5-ylboronic acid **46**	0.00046	0.080		0.0047	0.33	0.0047	0.55	5
6	1-n-Bu-2-phenyl-benzimidazole boronic acid **47**	9.26E-05	0.027		0.00093	0.066	0.00094	0.11	1
9	(3-aminophenyl)boronic acid pinacol ester **48**	9.26E-05	0.020		0.00093	0.066	0.00094	0.11	1
10	2-(N(iPr)₂-methyl)phenylboronic acid **49**	9.26E-05	0.019		0.00093	0.066	0.00094	0.11	1
11	Diisopropyl amine	0.00046	0.047		0.0046	0.33	0.0047	0.55	5
12	Benzene boronic acid	0.00046	0.056		0.0046	0.33	0.0047	0.55	5
13	Diisopropylethylamine	0.00046	0.060		0.0046	0.33	0.0047	0.55	5
14	Triethylamine	0.00046	0.047	0.065	0.0046	0.33	0.0047	0.55	5
15	Tri-n-butyl amine	0.00046	0.086	0.11	0.0046	0.33	0.0047	0.55	5
16	1,2-Diaminocyclohexane (mixed isomers)	0.00046	0.053	0.057	0.0046	0.33	0.0047	0.55	5
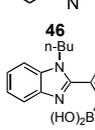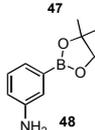
Synthesis of 2-methyl-*N*-[(1*S*)-1-phenylethyl]propanamide
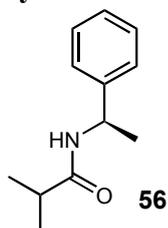
A mixture of (*R*)-α-methylbenzylamine (0.5 mL, 0.0039 moles), triethylamine (0.54 mL, 0.0039 moles) and dry ether (20 mL) was treated with isobutyryl chloride (0.4 mL, 0.0039 moles) dropwise over 1 minute. After 18 hours, the mixture was basified to pH 14 with dilute aqueous sodium hydroxide (10% w/w), the mixture was extracted with DCM (2 × 15 mL), the combined extracts

were dried (MgSO$_4$) and evaporated to give the amide (0.68 g, 91%) as a white powder which was used directly without further purification;

mp 94-96 °C; (Found C, 74.96; H, 9.01; N, 7.40%. C$_{12}$H$_{17}$NO requires C, 75.35; H, 8.96; N, 7.32%); δ$_H$(300 MHz, CDCl$_3$) 1.14 and 1.16 (each 3H, d, J = 6.6 Hz, CH.Me_2), 1.48 (3H, d, J = 6.9 Hz, Ar.CH.Me), 2.34 (1H, sept., J = 6.6 Hz, CH.Me$_2$), 5.12 (1H, quin., J = 6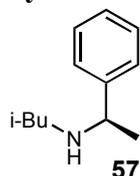.9 Hz, Ar.CH.Me), 5.64 (1H, br s, NH), 7.24-7.37 (5H, m, Ar) (addition of D$_2$O caused the signal at δ 5.64 to disappear and the signal at δ 5.12 to simplify to a t, J = 6.9 Hz); δ$_C$ (100 MHz, CDCl$_3$) 19.6 (2 x COCH(CH$_3$)$_2$), 21.7 (ArCHCH_3). 35.7 (COCH(CH$_3$)$_2$), 48.4 (ArCH), 126.1 (Ar), 127.3 (Ar), 128 (Ar), 143.4 (Ar), 175.9 (CO); m/z 223 (M+, +MeOH), 191, 149, 121, 115, 88

Synthesis of *N*-isobutyl-*N*-(1-phenylethyl)amine

A mixture of amide **2** (0.2 g, 0.001 moles) and dry THF (30 mL) was treated with dropwise addition over 5 minutes of borane-dimethylsulfide (2 M in THF, 9.4 mL, 0.018 moles) under an argon atmosphere and refluxed for 6 days. The reaction was quenched with water (2 mL) and acidified to pH=1 with 20% HCl and left to stir for 4 hours, aqueous layer was extracted with DCM (2 × 20 mL). The aqueous layer was then adjusted to pH=14 (5 mL, 20% NaOH) and extracted with DCM (2 × 20 mL) and EtOAc (1x30 mL). All the organic extracts were combined and dried (MgSO$_4$) and concentrated to yield a pale yellow oil, crude mass recovery 82 mg that was subjected to flash chromatography (100% DCM eluent, then 50:50 DCM:MeOH) to give a pale yellow oil, 40 mg, 14%

δ$_H$ (400 MHz, CDCl$_3$): 0.88 (dd, 6H, J = 4.4, 2.0 Hz, CH(CH_3), 1.37 (d, 3H J = 6.4 Hz, PhCHCH_3), 1.68-1.76 (m, 1H, CH(CH$_3$)$_2$), 2.19-2.37 (m, 2H, NCH_2), 3.76 (q, 1H J = 6.8 Hz, CHPh), 7.22-7.35 (m, 5H, Ph); δ$_C$ (100 MHz, CDCl$_3$): 20.6 (2 x CHCH_3), 24.3 (CHCH_3), 28.3 (CH(CH$_3$)$_2$), 55.7 (CHCH$_3$), 58.4 (NCH$_2$), 126.6 (Ph), 126.9 (Ph), 128.4 (Ph); IR: 1712 (s), 1533, 1471, 1429, 1366, 1133, 1080; m/z 209 (M+, + MeOH), 149, 122, 101, 74

Catalyst screening for attempted non-racemic synthesis of 43

A mixture of chloroform (5 mL), catalyst (see Table 2) (10 mol%) and *trans*-2-hexenal (0.61 mL, 0.0052 moles) was treated with thioacetic acid (0.33 mL, 0.0047 moles). After 3 hours, the reaction was quenched with dilute aqueous sodium hydroxide (5 mL of a 5% w/w solution), the organic layer

was separated, washed with dilute aqueous hydrochloric acid (3 mL of a 5% solution) and the crude organic extract was used directly for chiral GC analysis. GC analysis was carried out using a Chirasil-Dex CB column GC analysis: Injector temperature, 120 °C; Column flow, 1 mL/min; split ratio, 1:20; Initial oven temperature 80 °C; then 100 °C at a rate of 5 °C/min; hold for 2 minutes, then 120 °C at a rate of 10 °C/min; hold for 2 minutes; then 150 °C at a rate of 10 °C/min; hold for 12 minutes.

Table 7

Catalyst	Moles	Mass (mg)	Vol (mL)
(R)-α-methylbenzylamine	0.00052		0.06
Bis-α-methylbenzylamine	0.00052		0.12
L-Proline	0.00052	60	
L-Spartiene	0.00052		0.12
(R)-Tol-Binap	0.00052		0.35
(R)-(+)-MeOBIPHEP	0.00052		0.30

Thermal characterisation of the Thermos flask.

a) Solvent at 0 ºC

Toluene (100 mL) pre-chilled to 0 °C was added to the Thermos flask (pre-chilled to 4 °C in a fridge) and the temperature was recorded over time.

b) Solvent at 30 ºC

Toluene (100 mL) pre-heated to 30 °C was added to the Thermos flask (at room temperature) and the temperature was recorded over time.

c) Solvent at 40 ºC

Toluene (100 mL) pre-heated to 40 °C was added to the Thermos flask (at room temperature) and the temperature was recorded over time.

Figure 6. Temperature *versus* time results for the Thermos flask characterisation.
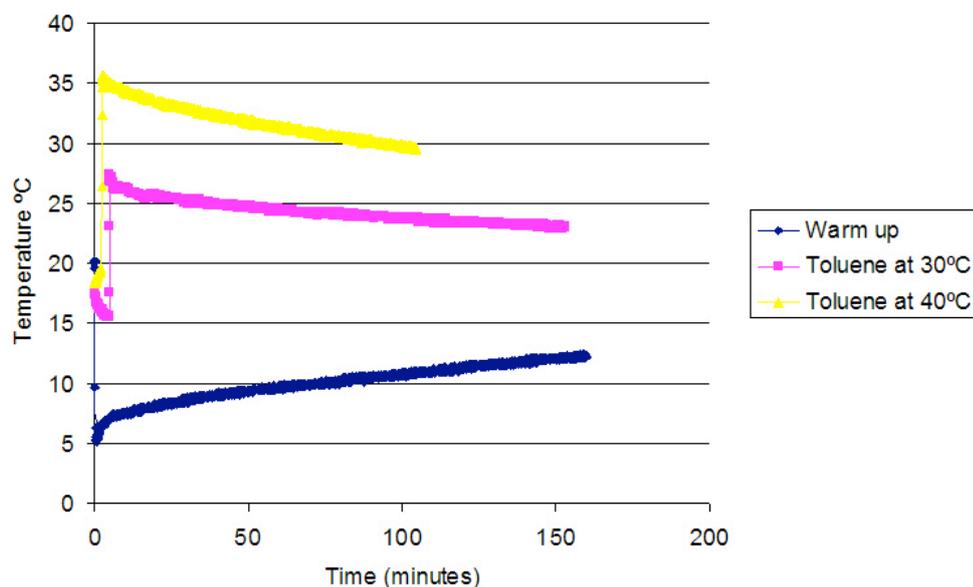
Low Temperature Study

Toluene (100 mL), *trans*-2-hexenal **42** (11.0 mL, 0.094 moles) and thioacetic acid **41** (6.6 mL, 0.094 moles) were each pre-weighed and cooled to -20 °C in the same cooling bath. The Thermos flask was also pre-chilled in the same cooling bath. The apparatus was quickly assembled, followed by the addition of toluene, **42** and **41** to the Thermos flask. Temperature changes were monitored over time.

Solvent Screening

Solvent (100 mL), *trans*-2-hexenal **42** (11.0 mL, 0.094 moles) and thioacetic acid **41** (6.6 mL, 0.094 moles) were added to the Thermos flask and the temperature change was recorded over time. Solvents employed were: 1) petroleum ether (80/100); 2) THF; 3) chloroform; 4) toluene; 5) DMF; 6) propiononitrile; 7) acetonitrile.

React IR Experiments

At t = 0 an air background was established, after t = 5 minutes chloroform (100 mL) was added, at t = 12 minutes *trans*-2-hexenal (11 mL, 0.094 moles) was added, at t = 67 minutes thioacetic acid (6.6 mL, 0.094 moles) was added, at t = 6 hours data collection was stopped. The ReactIR data was then analysed using the ConcIRT add-in to generate concentration profiles and subsequently infer the corresponding IR spectra.

General experimental procedure for the reaction of thioacetic acid with crotonaldehyde

A solution of crotonaldehyde 4 (62 μL, 0.0075 moles, 1.0 equiv.) and DCM (48 μL, 0.0075 moles, 1.0 eq.) in toluene-d8 (586 μL) was prepared and analysed by ^{1}H NMR spectroscopy. Thioacetic acid (54 μL, 0.75 mmol, 1.0 eq) was then added to the reaction solution and the sample was monitored by ^{1}H NMR spectroscopy for up to 9.5 hours. Once the data were assigned to corresponding species, the reaction profiles were obtained

Synthesis of 3-(benzylsulfanyl)hexanal
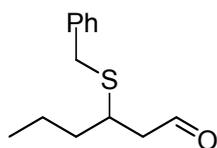
To a mixture of *trans*-2-hexenal (0.5 mL, 0.004 moles), triethylamine (0.1 mL), and DCM (20 mL), benzyl mercaptan (0.5 mL, 0.004 moles) was added. The mixture was stirred for 4 days. After dilution with DCM (20 mL) the organic phase was washed with dilute aqueous NaOH (20 mL, 10% w/w), dilute aqueous hydrochloric acid (20 mL 5%) and dried (MgSO$_4$) and concentrated to give a yellow oil. The oil was subjected to column chromatography (100% DCM eluent) to yield a clear liquid, 550 mg, 61.8%.

δ_H (400 MHz, CDCl$_3$): 0.79 (t, 3H, *J* = 7.4 Hz, *CH$_3$*), 1.31-1.37 (CH$_3$*CH$_2$*, m, 2H), 1.51-154 (CH$_3$CH$_2$*CH$_2$*, m, 2H), 2.47-2.58 (*CH$_2$*CHO, m, 2H), 2.95 (quintet, 1H, *J* = 6.8 Hz, SC*H*), 3.68, (s, 2H, SC*H$_2$*Ar), 7.17-7.26 (m, 5H, *Ar*), 9.58 (t, 1H, *J* = 2.0 Hz, C*H*O); δ_C (100 MHz, CDCl$_3$): 13.7 (*CH$_3$*), 19.9 (CH$_3$*CH$_2$*), 35.4(*CH$_2$*S), 37.3 (*CH$_2$*CH), 38.9 (CH$_2$*CH*), 48.7 (*CH$_2$*CHO), 127.1 (*Ar*), 128.6 (2 × *Ar*), 128.9 (2 × *Ar*), 133.2 (*Ar*), 201.0 (*CHO*); IR: 1725(s), 1677(m), 1629(m), 1492, 1453, 1266, 1124; m/z 254 (M+, + MeOH), 196, 176, 148, 116

Synthesis of methyl 3-(benzylsulfanyl)-3-phenylpropanoate:
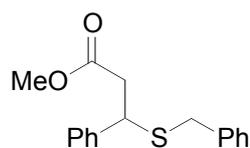
To a mixture of methyl cinnamate (1.13 g, 0.007 moles), Hünig's base (0.1 mL), and EtCN (20 mL), benzyl mercaptan (0.82 mL, 0.007 moles) was added. The reaction mixture was stirred for 4 days at reflux. After dilution with DCM (20 mL) the organic phase was washed with dilute aqueous NaOH (20 mL, 10% w/w), dilute aqueous hydrochloric acid (20 mL 1 M) and dried (MgSO$_4$) After evaporation purification by silica gel chromatography (100 % DCM as eluent) yielded a pale yellow liquid, 1.69g, 84%

δ_H (400 MHz, CDCl$_3$): 2.72-2.83 (m, 2H, CH*CH$_2$*), 3.50 (s, 3H, O*Me*), 3.74 (s, 2H, S*CH$_2$*), 4.09 (t, 1H, *J* = 8.4 Hz, *CH*S), 7.20-7.31 (m, 10H, 2 x *Ph*); δ_C (100 MHz, CDCl$_3$): 35.7 (*CH$_2$*CO), 41.3 (*CH$_2$*S), 45.0 (O*Me*), 51.7 (*CH*S), 127.8-129.4 (12 x Ph), 171.0 (*CO*); IR: 1736, 1604, 1496, 1453, 1441, 1362, 1338, 1220, 1153, 1077; m/z 318 (M+, + MeOH), 256, 242, 210, 196, 164, 124

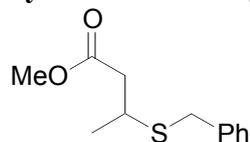**Synthesis of methyl 3-(benzylsulfanyl)butanoate:**

To a mixture of methylcrotonate (0.74 mL, 0.007 moles), Hünig's base (0.1 mL), and EtCN (20 mL), benzyl mercaptan (0.82 mL, 0.007 moles) was added. The reaction was stirred for 4 days at reflux. After dilution with DCM (20 mL) the organic phase was washed with dilute aqueous NaOH (20 mL, 10%), dilute aqueous hydrochloric acid (20 mL 5%) and dried (MgSO$_4$) After evaporation and purification by silica gel chromatography (DCM as eluent) to yield a pale yellow liquid, 88%, 1.40 g

δ_H (400 MHz, CDCl$_3$): 1.23 (d, 3H, J = 6.8Hz, *CH$_3$*CH), 2.34-2.58 (m, 2H, CH*CH$_2$*), 3.05 (sextet, 1H, J = 7.2Hz, *CH*CH$_2$), 3.60 (s, 3H, O*CH$_3$*), 3.70 (s, 2H, *CH$_2$*S), 7.15-7.28 (m, 5H, *Ph*);δ_C (100 MHz, CDCl$_3$): 21.2 (*CH$_3$*CH), 35.4 (*CH$_2$*S), 36.0 (CH$_3$*CH*), 41.9 (*CH$_2$*CO), 51.7 (O*CH$_3$*), 127.0 (Ph), 128.7 (Ph), 138.2 (Ph), 171.79 (*CO*); IR: 1738, 1499, 1455, 1355, 1305, 1167; All spectral data agree with literature precedent[74]

Investigation of addition of thioacetic acid to cinnamaldehyde

React-IR

At t = 0 an air background was established, after t = 12 minutes toluene (25 mL) was added, at t = 36 minutes cinnamaldehyde (2.91 mL, 0.023 moles) was added, at t = 50 minutes thioacetic acid (1.65 mL, 0.023 moles) was added, at t = 6 hours data collection was stopped. The ReactIR data were then analysed using the ConcIRT add-in to generate concentration profiles and subsequently infer the corresponding IR spectra.

Adiabatic Calorimetry

Toluene (100 mL), cinnamaldehyde (11.62 mL, 0.094 moles) and thioacetic acid   (6.6 mL, 0.094 moles) were added to the Thermos flask and the temperature change was recorded over time.

Investigation of the addition of thioacetic acid to trans-nitrostyrene:

Adiabatic Calorimetry

Toluene (100 mL), trans-nitrostyrene (13.77 g, 0.094 moles) and thioacetic acid   (6.6 mL, 0.094 moles) was added to the Thermos flask and the temperature change was recorded over time.

React IR:

At t = 0 an air background was established, after t = 20 minutes toluene (25 mL) was added, at t = 38 minutes *trans*-nitrostyrene (1.3 g, 0.023 moles) were added, at t = 51 minutes thioacetic acid (1.65 mL, 0.023 moles) was added, at t = 6 hours data collection was stopped. The ReactIR data were then analysed using the ConcIRT add-in to generate concentration profiles and subsequently infer the corresponding IR spectra.

Figure 1 Key: Going left to right:

Red = chloroform, Green = nitrostyrene, turquoise = Thioacid, purple, pink, grey, blue - not assigned

Investigation of Thioacetic acid addition to methyl crotonate

Adiabatic Calorimetry

Toluene (100 mL), methyl crontonate (9.25 mL, 0.094 moles) and thioacetic acid (6.6 mL, 0.094 moles) were added to the Thermos flask and the temperature change was recorded over time.

React-IR

At t = 0 an air background was established, after t = 3 minutes toluene (25 mL) was added, at t = 12 minutes methyl crotonate (2.25 mL, 0.023 moles) was added, at t = 22 minutes thioacetic acid (1.65 mL, 0.023 moles) was added, at t = 6 hours data collection was stopped. The ReactIR data was then analysed using the ConcIRT add-in to generate concentration profiles and subsequently infer the corresponding IR spectra.

69

Investigation of the addition of benzyl thiol to methyl crotonate

At t = 0 an air background was established, after t = 15 minutes toluene (25 mL) was added, at t = 12 minutes methyl crotonate (2.25 mL, 0.023 moles) was added, at t = 22 minutes benzyl thiol (2.71 mL, 0.023 moles) was added, at t = 6 hours data collection was stopped. The ReactIR data was then analysed using the ConcIRT add-in to generate concentration profiles and subsequently infer the corresponding IR spectra.

Adiabatic Calorimetry

Toluene (100 mL), methyl crontonate (9.25 mL, 0.094 moles) and benzyl thiol (11.5 mL, 0.094 moles) was added to the Thermos flask and the temperature change was recorded over time.

Investigation of addition of benzyl thiol to trans-nitrostyrene

React-IR

At t = 0 an air background was established, after t = 16 minutes toluene (25 mL) was added, at t = 31 minutes *trans*-nitrostyrene (3.44 g, 0.023 moles) was added, at t = 62 minutes benzyl thiol (2.71 mL, 0.023 moles) was added, at t = 6 hours data collection was stopped. The ReactIR data was then analysed using the ConcIRT add-in to generate concentration profiles and subsequently infer the corresponding IR spectra.
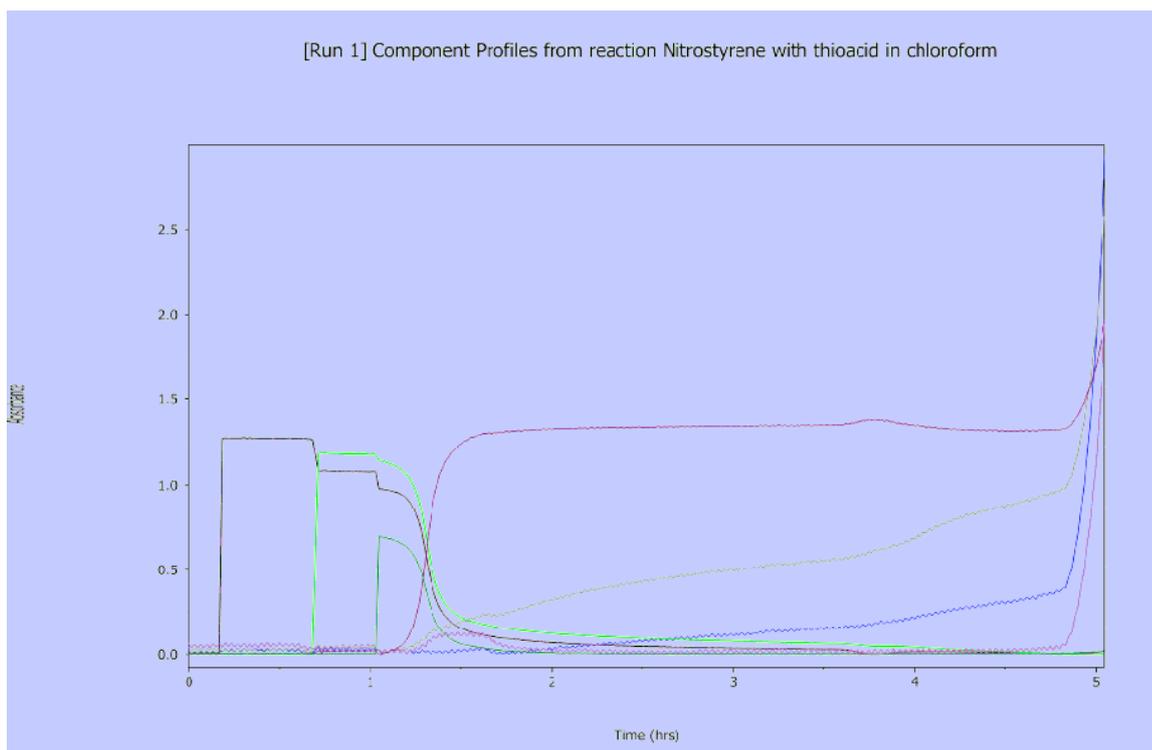
Adiabatic Calorimetry

Toluene (100 mL), *trans*-nitrostyrene (13.77 g, 0.094 moles) and benzyl thiol (10.83 mL, 0.094 moles) was added to the Thermos flask and the temperature change was recorded over time.

Investigation of addition of benzyl thiol to methyl cinnamate

React-IR

At t = 0 an air background was established, after t = 16 minutes toluene (25 mL) was added, at t = 31 minutes methyl cinnamate (3.74 g, 0.023 moles) was added, at t = 62 minutes benzyl thiol (2.71 mL, 0.023 moles) was added, at t = 6 hours data collection was stopped. The ReactIR data was then analysed using the ConcIRT add-in to generate concentration profiles and subsequently infer the corresponding IR spectra.

Adiabatic Calorimetry

Toluene (100 mL), methyl cinnamate (14.98 g, 0.094 moles) and benzyl thiol (10.83 mL, 0.094 moles) was added to the Thermos flask and the temperature change was recorded over time.

Investigation of amine based catalysis

Adiabatic Calorimetry

Toluene (100 mL), thioacetic acid (6.6 mL, 0.094 moles) and Hünig's base (16.09 mL, 0.094 moles) was added to the Thermos flask and the temperature change was recorded over time. At t = 29 minutes the contents were removed from the flask, cooled to 25 ºC in a water bath and returned to the thermos flask, at

t = 33 minutes *trans*-2-hexenal (10.71 mL, 0.094 moles) was added to the Thermos flask and the temperature change was recorded over time.

DMSO screening experiments

Initial Observation

DMSO (100 mL) and hexenal (11 mL, 0.094 moles) thioacetic acid (6.6mL, 0.094moles) was added to the thermos flask and the temperature rise was recorded over time, after the reaction reached ambient temperature solid had precipitated, Mp 119 ºC; (Found C, 0 H, 0; N, 0%. S_8 requires C, 0; H, 0; N, 0%); M/S (EI) 256 ;

NMR experiment

d_6 DMSO (0.75 mL) and thioacetic acid (0.0495 mL, 0.00071moles) was added to an NMR tube and the ^{13}C NMR spectra recorded every 5 minutes for 30 minutes, then every 20 minutes for a total time of 90 minutes. Thioacetic acid, DMSO and dimethylsulfide correspond to literature values.

NMR experiment

d_6 DMSO (0.75 mL) and hexenal (0.0825 mL, 0.00071 moles) thioacetic acid (0.0495 mL, 0.00071moles) was added to an NMR tube and the ^{13}C NMR spectra recorded every 5 minutes for 30

minutes, then every 20 minutes for a total time of 90 minutes. Thioacetic acid, DMSO, *trans*-2-hexenal and dimethylsulfide correspond to literature values.

NMR experiment

CDCl$_3$ (0.75 mL) and hexenal (0.0825 mL, 0.00071 moles) thioacetic acid (0.0495 mL, 0.00071 moles) was added to an NMR tube and the ^{13}C NMR spectra recorded every 5 minutes for 30 minutes, then every 20 minutes for a total time of 90 minutes. Thioacetic acid, d$_6$-DMSO, *trans*-2-hexenal and dimethylsulfide correspond to literature values.

ReactIR Studies, chloroform

Machine was baseline corrected, and chloroform (50 mL) added, left for 5 minutes to establish a further baseline, thioacetic acid (4.9 mL, 0.07 moles) leaving for 5 minutes to establish a baseline, followed by DMSO (5.0 mL, 0.07 moles). After 3 hours the mixture turns cloudy and after 12 hours was biphasic (chloroform was the bottom layer), after a further 72 hours elemental sulfur precipitates – 0.37 g, 16%.

ReactIR studies, toluene

Machine was baseline corrected, and toluene (50 mL) added, left for 5 minutes to establish a further baseline, thioacetic acid (4.9 mL, 0.07moles) leaving for 5 minutes to establish a baseline, followed by DMSO (5.0 mL, 0.07 moles), mixture turns cloudy and biphasic (toluene is top layer), after a further 72 hours elemental sulfur precipitates – 0.37g, 16%.

ReactIR studies, neat (solventless) reaction

Machine was baseline corrected, thioacetic acid (20 mL, 0.29 moles) was added followed by DMSO (20 mL, 0.29 moles), violent exotherm, after 3 days elemental sulfur precipitated 2.16 g, 23%.

4.0 References

[1] a) P. Ball, *Chemistry World*, **3**, 2006, "Chancing Upon Chemical Wonders"; b) Pliny the Elder, *Natural History*.

[2] G. Whitesides, 'Chemistry at the Centre: an International Assessment of University Research in Chemistry in the UK'. The international review was co-ordinated by the Royal Society of Chemistry on behalf of EPSRC and took place in 2002.

[3] A.R. Wright, "The Road to Gold", Process Chemistry & Engineering - Working together in isolation, 10-12 April 2006, RSC, Newcastle Civic Centre.

[4] a) T. Laird, *Org. Process Res. Dev.*, **12**, 2007, Editorial article; b) Bretherick's Handbook of Reactive Chemical Hazards, 7th Ed, ISBN 0123725631.

[5] Harsnet, Thematic Network on Hazard Assessment of Highly Reactive Systems, http://www.iqs.url.es/harsnet. Industrial and Materials Technologies Programme of the European Commission; Project BET2-0572.

[6] N.N. Semenov, *Z Phys. Chem.*, **1928**, *48*, 571-579.

[7] Frank Kamenetskii, DA, **1989**, *Diffusion and heat transfer in chemical Kinetics*, 2nd Edition (Plenum Press, London, UK).

[8] D.I. Townsend, J.C. Tou, *Thermochim. Acta*, **1980,** *37*, 1-30.

[9] a) L. Boymond, M. Rottlander, G. Cahiez, P Knochel, *Agnew. Chem. Int. Ed.*, **1998**, *37*, 1701-1711 b) A.E. Jensen, W. Dohle, I. Sapountzis, D.M. Lindsay, A.V. Vu, P. Knochel, *Synthesis*, **2002**, *4*, 565-572 c) P. Knochel, W. Dohle, N. Gommermann, F.F. Kneisel, F. Kopp, T. Korn, I. Sapountzis, V.A. Vu, *Agnew. Chem. Int. Ed.*, **2004**, *43*, 4302-4311.

[10] J.T. Reeves, M. Sarvestani, J.J. Song, Z. Tan, L.J. Nummy, H. Lee, N.K. Yee, C.H. Senanayake, *Org. Process Res. Dev.,* **2006**, *10*, 1258-1262.

[11] W. Dermaut, *Org. Process Res. Dev.*, **2006**, *10*, 1251-1257.

[12] I Eskendirov, B. Kabongo, L. Glasser, V.D. Sokolovoskii, *J. Chem. Soc. Faraday Trans.*, **1995**, *91*, 991-994.

[13] S.R. Maple, A. Allerhand, *J. Am. Chem. Soc.*, **1987**, *109*, 6609-6613.

[14] a) A.A. Frost, R.G. Pearson, *Kinetics and Mechanism*, 2nd Ed, Wiley, New York, 1961, ch. 12, pp 335-350 b) K. Koelichen, *Z. Phys. Chem.*, **1900**, *33*, 129-130 c) C.C. French, *J. Am. Chem. Soc.*, **1929**, *51*, 3215-3221 d) V.K. La Mer, M.L. Miller, *J. Am. Chem. Soc.*, **1935**, *57*, 2674-2681.

[15] A. Akao, N. Nonoyama, T. Mase, N. Yasuda, *Org. Process Res. Dev*, **2006**, *10*, 1178-1183.

[16] A. Akao, K. Sato, N. Nonoyama, T. Mase, N. Yasuda, *Tetrahedron Lett.*, **2006**, *47*, 969-972.

[17] M. Klussmann, H. Iwamura, S.P. Mathew, D.H. Wells Jr., U. Pandya, A. Armstrong, D.G. Blackmond, *Nature*, **2006**, *441*, 621-623.

[18] S.P. Mathew, H. Iwamura, D.G. Blackmond, *Agnew. Chem. Int. Ed.,* **2004**, *43*, 3317-3321.

[19] J. Le Bars, T. Haubner, J. Lang, A. Pfaltz, D.G. Blackmond, *Adv. Synth. Catal.*, **2001**, *343*, 207-214.

[20] a) A. Michael, *J. Am. Chem. Soc.*, **1887**, *9*, 112-119; b) A. Michael, *Prakt. Chem.*, **1887**, *35*, 349-356; c) T. Komnenos, *Ann. Chem.*, **1883**, *218*, 145-169; d) N. Sokoloff, P. Latschinoff, *Ber. Dtsch. Chem. Ges*, **1874**, *7*, 1384-1387; e) F. Loydl, *Ann. Chem.*, **1883**, *192*, 80-88.

[21] a) J. Leonard, E. Diez-Barra, S. Merino, *Eur. J. Org. Chem.*, **1998**, 2051-2061; b) B. E.Rossiter, N. M.Swingle, *Chem. Rev.*, **1992**, *92*, 771-806.

[22] a) S. Hoz, *Acc. Chem. Res.*, **1993**, *26*, 69-74; b) A. Kina, H. Iwamura, T. Hayashi, *J. Am. Chem. Soc.*, **2006**, *128*, 3904-3905; c) H. K. Oh, I. K. Kim, H. W. Lee, I. Lee, *J. Org. Chem.*, **2004**, *69*, 3806-3810.

[23] a) T. C. Waqbnitz, J.-Q. Yu, J. B. Spencer, *Chem. Eur. J.*, **2004**, *10*, 484-493; b) T. C. Wabnitz, J. B. Spencer, *Org. Lett.*, **2003**, *5*, 2141-2144; c) L. Yang, L.-W. Xu, C.-G. Xia, *Tetrahedron Lett.*, **2005**, *46*, 3279-3282;

[24] J. Seayad, B List, *Org. Biomol. Chem.*, **2005**, *3*, 719–724.

[25] a) H. Pracejus, *Justus Liebigs Ann. Chem.*, **1960**, *634*, 9–22; (b) H. Pracejus, *Justus Liebigs Ann. Chem.*, **1960**, *634*, 23–29; (c) Z.G.Hajos, D. R. J. Parrish, *J. Org. Chem.*, **1974**, *39*, 1615–1621; (d) U. Eder, G. Sauer, R. Wiechert, *Angew. Chem., Int. Ed.*, **1971**, *10*, 496–497.

[26] a) P. I. Dalkoand, L. Moisan, *Angew. Chem., Int. Ed.*, **2001**, *40*, 3726–3748; (b) A. Berkessel, H. Groger, *Asymmetric Organocatalysis, VCH, Weinheim*, 2004.

[27] PI. Dalko, L. Moisan *Angew. Chem. Int. Ed.*, **2004**, *43*, 5138 − 5175.

[28] J.L. Tucker, *Org. Process Res. Dev.*, **2006**, *10*, 315-319.

[29] a) A. Michael, *J. Am. Chem. Soc.*, **1887**, *9*, 112-119 b) A. Michael, *Prakt. Chem*, **1887**, *35*, 349-356 c) T. Komnenos, *Justus Leibigs Ann. Chem*, **1883**, *218*, 145-169 d) N. Sokoloff, P. Latschinoff, *Ber. Dtsch. Chem. Ges*, **1874**, *7*, 1384-1387 e) F. Loydl, *Justus Leibigs Ann. Chem.* **1883**, *192*, 80-88

[30] a) J. Leonard, E. Diez-Barra, S. Merino, *Eur. J. Org. Chem.*, **1998**, 2051-2061.
b) B. E. Rossiter, N. M. Swingle, *Chem. Rev.*, **1992**, *92*, 771-806.
c) B. H. Kim, H. B. Lee, J. K. Hwang, Y.G.Kim, *Tetrahedron Asymmetry*, **2005**, *16*, 1215-1220.

[31] a) D. P. Curran, L.H.Kuo, *Tetrahedron Lett.*, **1995**, *36*, 6647-6650 b) P.R. Schreiner, A. Wittkopp, *Org. Lett.*, **2002**, *4*, 217-220 c) P.R. Schreiner, A. Wittkopp, *Chem. Eur. J.*, **2003**, *9*, 407-414 d) P. Vachal, E.N. Jacobsen, *Org. Lett.*, **2000**, *2*, 867-870 e) P. Vachal, E.N. Jacobsen, *J. Am. Chem. Soc.*, **2002**, *124*, 10010-10014 f) A. Wenzel, E.N. Jacobsen, *J. Am. Chem. Soc.*, **2002**, *124*, 12964-12965 g) T. Okino, Y. Hoashi, Y. Takemoto, *Tetrahedron Lett.*, **2003**, *44*, 2817-2821 h) T. Okino, Y. Hoashi, Y. Takemoto,*J. Am. Chem. Soc.*, **2003**, *125*, 12672-12673.

[32] Y. Sohtome, A. Tanatani, Y. Hashimoto, K. Nagasawa, *Chem. Pharm. Bull.*, **2004**, *52*, 477-480.

[33] M.P. Lalonde, Y. Chen, E.N. Jacobsen, *Agnew. Chem. Int. Ed.*, **2006**, *45*, 6366-6370.

[34] S. Mukherjee, J. W. Yang, S. Hoffmann, B. List, *Chem. Rev.*, **2007**, *107*, 5471-5569.

[35] B. List, P. Pojarliev, H.J. Martin, *Org. Lett.*, **2001,** *3*, 2423-2425.

[36] Y. Hayashi, H. Gotoh, T. Hayashi, M. Shoji, *Agnew. Chem. Int. Ed.*, **2005**, *44*, 4212-4215.

[37] M.A. Ghannoum, L.B. Rice, *Clin. Microbiol. Rev.*, **1999**, *12*, 50-69.

[38] P. Diner, M. Nielson, M. Marigo, K.A. Jorgenson, *Agnew. Chem. Int. Ed.*, **2007**, *46*, 1983-1987.

[39] M. Marigo, T. Schulte, J. Franzen, K.A. Jorgenson, *J. Am. Chem. Soc.*, **2005**, *127*, 15710-15711

[40] P. Bernal, J. Tamariz, *Tetrahedron Lett.*, **2006**, *47*, 2905-2909.

[41] A. Alexakis, O. Andrey, *Org. Lett.*, **2002**, *4*, 3611-3614.

[42] A. Alexakis, S. Mosse, *Org. Lett.*, 496-497.

[43] H. Li, J. Wang, L. Zu, W. Wang, *Tetrahdron Lett.*, **2006**, *47*, 2585-2589.

[44] J. Wang, H. Li, L. Zu, W. Wang, *Org. Lett.*, **2006**, *8*, 1391-1394.

[45] B.H. Kim, H.B. Lee, J.K. Hwang, Y.G. Kim, *Tetrahedron Asymm.*, **2005**, *16*, 1215-1220.

[46] A. Ortiz, H. Hernandez, G. Mendoza, L. Quintero, S. Bernes, *Tetrahedron Lett.*, **2005**, *46*, 2243-2246.

[47] A.G. Schultz, Y.K. Yee, *J. Org. Chem.*, **1976**, *41*, 4044-4051.

[48] A. Kamimura, N. Murakami, F. Kawahara, K. Yokota, Y. Omata. K. Matsuura, Y. Oishi, R. Morita, H. Mitsudera, H. Suzukawa, A. Kakehi, M. Shirai, H. Okamoto, *Traherdron*, **2003**, *59*, 9537-9546.

[49] M.C. Carreno, *Chem. Rev.*, **1995**, *95*, 1717-1760.

[50] a) G.H. Posner, P.W. Tang, J.P. Mallamo, *Tetrahedron Lett.*, **1978**, *42*, 3995-3998 b) H. Okamura, Y. Mitsuhira, M. Miura, H. Yakei, *Chem. Lett.*, **1978**, 517-520.

[51] a) J. Fawcett, S. House, P.R. Jenkins, N.J. Lawrence, D.R. Russell, *J. Chem. Soc., Perkin Trans. 1*, **1993**, 67-73 and references therein b) R.K. Haynes, A.G. Katsifis, *Aust. J. Chem.*, **1989**, *42*, 1473-1483 c) R.K. Haynes, A.G. Katsifis, *J. Chem. Soc. Chem. Commun.*, **1987**, 340-342.

[52] G. Solladie, G. Moine, *J. Am. Chem. Soc.*, **1984**, *106*, 6097-6098.

[53] N. Maezaki, S. Yuyama, H. Sawamoto, Y. Suzuki, M. Izumi, T. Tanaka, *Org. Lett.*, **2001**, *3*, 29-31.

[54] N. Maezaki, S. Yuyama, H. Sawamoto, Y. Suzuki, M. Izumi, R. Yoshigami, H. Ohishi, T. Tanaka, *J. Org. Chem.*, **2004**, *69*, 6335-6340.

[55] G. Kumuraswamy, M.N.V. Sastry, N. Jena, *Tetrahedron Lett.*, **2001**, *42*, 8515-8517.

[56] E. A. Schmittling, J.S. Sawyer, *Tetraherdon Lett.*, **1991**, *32*, 7207.

[57] L. Yang, L.W Xu, C.G. Xia, *Tetrahedron Lett.*, **2005**, *46*, 3279-3282.

[58] M. Kawatsura, J.F. Harwig, *Organometallics*, **2001**, *20*, 1960-1964.

[59] I. Reboule, R. Gil, J. Colin, *Tetrahedron Lett.*, **2005**, *46*, 7761-7764.

[60] H. Sasai, T. Suzuki, S. Arai, T. Arai, M. Shibasaki, *J. Am. Chem. Soc.*, **1992**, *114*, 4418.

[61] N. Yamagiwa, H. Qin, S. Matsunaga, M. Shibasaki, *J. Am. Chem. Soc.*, **2005**, *127*, 13419-13427.

[62] S. K. Garg, R. Kumar, A.K. Chakraborti, *Tetrahedron Lett.*, **2005**, *46*, 1721-1724.

[63] M. L. Kantam, B. Neelima, Ch.V. Reddy, *J. Mol. Cat. A: Chemical*, **2005**, *241*, 147-150.

[64] M. Kumarraja, K. Pitchumani, *J. Mol. Cat. A: Chemical*, **2006**, *256*, 138-142.

[65] B. M. Fetterly, N.K. Jana, J.G. Verkade, *Tetrahedron*, **2006**, *62*, 440-456.

[66] A. Strecker, *Ann. Chem. Pharm.*, **1850**, *75*, 27-32.

[67] B. Das, N. Chowdhury, K. Damodar, *Tetrahedron Lett.*, **2007**, *48*, 2867-2870.

[68] S. Hussain, S.K. Bharadwaj, M. K. Chaudhuri, H. Kalita, *Eur. J. Org. Chem.*, **2007**, 347-378.

[69] a) F. Robert, J. Heritier, J. Quiquerez, H. Simian, I. J. Blank. *J. Agric. Food Chem.* **2004,** *52,* 3525-3529. b) S. Widder, C. S. Luntzel, T. Dittner, W. Pickenhagen, J. *Agric. Food Chem.* **2000,** *48,* 418-423.

[70] H. Wakabayashi, M. Wakabayashi, W. Eisenreich, K-H. Engel, *J. Agric. Food Chem.* **2003**, *15*, 4349-4355.

[71] C. L. Arcus, D. G. Smyth *J. Chem. Soc.* **1955**, 34-40.

[72] D. Enders, K. Luttgen, A. Narine, *Synthesis* **2007**, *7*, 959-980.

[73] a) R. L. Giles, J. A. K. Howard, L. G. F. Patrick, M. R. Probert, G. E. Smith, A. Whiting, *J. Organomet. Chem.* **2003**, *680*, 257; b) S. W.Coghlan, R. L. Giles, J. A. K. Howard, M. R. Probert, G. E. Smith, A. Whiting, *J. Organomet. Chem.* **2005**, *490*, 4784; c) K. Arnold, B. Davies, R. L. Giles, C. Grosjean, G. E. Smith, A. Whiting, *Adv. Synth. Catal.*, **2006**, *348*, 813-820.

[74] I. Kumar, R. S. Kolly, *Org. Lett.*, **1999**, *1*, 207-209, b) I. Kumar, R.S. Jolly, *Org Lett.*, **2001**, *3*, 283-285.